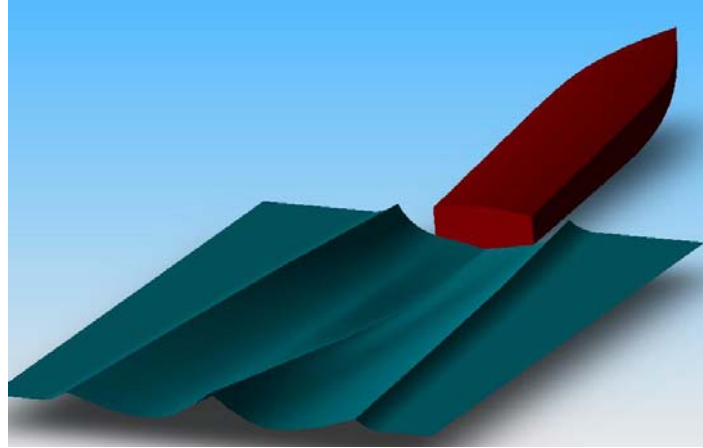


Surface Wave Contours Associated with the Forebody Wake of Stepped Planing Hulls

Author Names: Daniel Savitsky¹ (Member) and Michael Morabito² (Associate Member)

1 Professor Emeritus, Davidson Laboratory, Stevens Institute of Technology

2 Research Engineer, Davidson Laboratory, Stevens Institute of Technology



Results of an extensive series of model tests that define the longitudinal surface wake profiles aft of prismatic hulls having deadrise angles of 10 °, 20 ° and 30 ° are presented. Empirical equations are developed that quantitatively define these profiles and are in a form that can be easily applied by designers of stepped planing hulls. These equations are applicable for an expected range of variations in trim angle, speed coefficient, and loading coefficient typical for these hulls. A brief introduction to the concept and to the hydrodynamic advantages of stepped planing hulls is presented to orient the reader as to the importance of wake data in their design. Examples are presented that illustrate the application of these wake data for stepped planing hulls with wetted forebody chine to achieve maximum hydrodynamic lift/drag ratios. Finally experimental results are presented that illustrate the potential resistance penalty associated with the operation of chines dry forebodies where the stagnation line crosses the step.

INTRODUCTION

The increasing availability of light-weight, high-horsepower engines has motivated the designers of planing craft to design for increases in maximum speed. It was soon realized however that the ubiquitous hard chine planing monohull configuration has inherent hydrodynamic characteristics that result in exponentially increasing resistance as the maximum design speed increases and thus quickly consumes the available horsepower.

An alternative high speed planing hull configuration is the stepped hull. It enables the designer to substantially reduce the hydrodynamic resistance at high speed (compared to an equivalent monohull) thus resulting in a more efficient utilization of the installed power. As will be described in detail in the subsequent section of this paper the stepped hull has a transverse discontinuity (step) located somewhat aft of mid-ship. This results in a forebody that planes on the oncoming free water surface and the flow separates from the bottom at the step. The afterbody interacts with the wake of the forebody. The combination of the forebody and afterbody

forces must provide for vertical equilibrium of the craft. While the force on the forebody can be readily calculated using published methods, the afterbody force is not readily calculated since it is dependent upon the shape of the forebody wake that may intersect the afterbody bottom. Unfortunately, there has been a dearth of published data that describes the forebody surface wake geometry.

This study reviewed surface wave data obtained from early studies of water-based aircraft (all have stepped hulls) and concludes that their parametric variations were not generally applicable to stepped planing craft. Consequently, it was necessary to conduct additional experimental studies of planing hull wakes at the Davidson Laboratory for test conditions more appropriate to planing craft. The results are presented in a form that is easily applied by the designers of stepped planing craft to select optimum step depth and afterbody trim orientation relative to the forebody and to estimate afterbody wetted areas.

Prior to the presentation of the wake results, and to provide further background for the use of stepped hull geometries, brief summaries are provided of the lift and drag characteristics of planing hulls; the limitations of the monohull at high speed;

and finally how the stepped hull overcomes these limitations. A hull configuration having a length of 32 ft (9.8m), a displacement of 10,000 lbs (4546 kg) and operating in the chines wetted condition is used to illustrate the results. Future studies of the chines dry operating condition, such as is common in multi-step high speed racing craft, are planned.

It is believed that this background may be useful in understanding the necessity for defining the forebody surface wake geometries in the design of stepped hulls.

IMPORTANCE OF TRIM ANGLE ON THE HYDRODYNAMIC RESISTANCE OF PLANING CRAFT

One of the most significant parameters that influence the performance of a planing craft is the equilibrium trim angle which varies with speed. It has a major effect on resistance, seakeeping, porpoising, and lateral stability. Each of these performance characteristics is worthy of a separate discussion. However, for the purposes of this paper only the effect of trim angle on hydrodynamic resistance is considered. It is shown that the particular relationship between trim and resistance naturally leads to adaptation of the stepped hull form at high planing speeds.

To best illustrate the dependence of resistance on trim angle, use is made of the planing lift and resistance equations for prismatic hulls from Savitsky (1964). These are repeated below:

Lift Coefficient of Zero Deadrise Surface:

$$C_{l_0} = \Delta / 0.50 \rho V^2 B^2 = \tau^{1.1} (0.120 \lambda^{1/2} + 0.0055 \lambda^{5/2} / C_V^2) \quad (1)$$

Lift Coefficient of Deadrise Surface:

$$C_{l_\beta} = C_{l_0} - 0.0065 \beta C_{l_0}^{0.60} \quad (2)$$

Hydrodynamic Resistance (exclusive of whisker-spray drag):

$$R_T = \Delta \tan \tau + 0.50 \rho V^2 \lambda B^2 C_f \quad (3)$$

For the purpose of this illustration, consider a planing craft that has the following geometry; loading and speed:

LOA =	32 ft (9.8 m)
Chine Beam (B) =	7.8 ft (2.4 m)
Deadrise angle (β) =	12.5°
Displacement (Δ) =	10,000 lbs (4546 kg)
Velocity (Vk) =	40 knots
C_{l_β} =	0.036
Roughness allowance =	0

Now consider the planing surface free to heave but running over a range of fixed trim angles. Using the above equations, the wetted area (λB^2) and the total resistance/ displacement

ratio (R_T/Δ) can be calculated as a function of trim angle. The results are plotted on Fig. 1. (Similar calculations can be made for other deadrise angles; width of beam; displacements; and speeds.) Although the absolute values of the results will be different, the general conclusions on the effects of trim angle on wetted area and total resistance/displacement ratio will be essentially similar to that shown on Fig. 1.

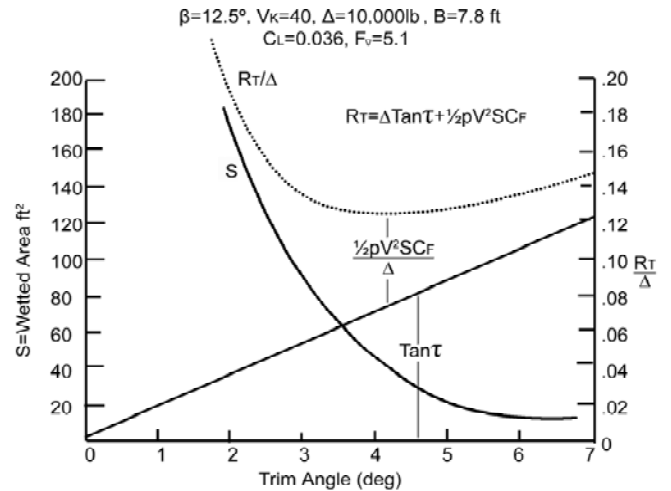


Fig. 1: Calculated Wetted Area and R_T/Δ vs. Trim Angle

Variation of Wetted Area with Trim Angle

Referring to Fig. 1 it is to be noted that the wetted surface area varies inversely as an exponential power of trim angle. For example, decreasing the trim angle from 4° to 2° nearly quadruples the wetted surface for a prismatic hull. This is significant since the viscous resistance component increases linearly with the size of the wetted area (neglecting the relatively small change in C_f as the wetted length increases). Further, for trim angles less than 5° there is a rapid increase in wetted area as the trim is decreased, while for larger trim angles there is only a moderate decrease in wetted surface as the trim increases.

Variation of R_T/Δ with Trim Angle

As is well known to designers of planing craft, the total hydrodynamic resistance (exclusive of whisker spray drag) is the sum of the pressure drag ($\Delta \tan \tau$) that increases with increasing trim angle and the viscous resistance developed by the wetted bottom area which decreases with increasing trim angle. For the current example, it is seen from Fig.1 that the sum of these two components attains a minimum value in the proximity of 4° and increases for smaller and larger trim angles. The trim angle for minimum resistance increases slightly as the deadrise angle is increased. For the present 12.5° deadrise angle it is seen that decreasing the trim angle from 4° to 2° will nearly double the hydrodynamic resistance. Practical hull forms have a longitudinally convex bow curvature that, if wetted at low trim angles, will add additional form resistance. Designers are certainly aware of this trim effect on resistance

and attempt to locate the LCG to achieve optimum trim angles and hence minimum resistance/displacement ratios. Of course this is not always achievable, particularly with high-speed planing monohulls. Some designers will introduce a “rocker” geometry at the transom in order to increase the running trim angle—but this alternation is usually not completely effective.

LIMITATIONS OF PLANING MONOHULLS AT HIGH SPEED

Using the planing monohull hull geometry and dimensions previously listed, but now locating the LCG at 14.4 ft forward of the transom and allowing the craft to have freedom in heave and trim, the equilibrium values of trim and resistance, as function of speed, can be calculated using the method from Savitsky (1964). These results are shown on Fig. 2. For the purpose of presenting a simple illustration, the added resistance due to the whisker spray (Savitsky, 2007) is omitted. This will not change the conclusions of the present discussion.

Trim Variation with Speed

Note from Fig.2 that, as is usual, the equilibrium trim angle decreases with increasing speed. At a planing speed of 20 knots, the trim angle is approximately 3° and, as shown on Fig.1, this results in an essentially minimum value of resistance/displacement ratio. As speed increases, the equilibrium trim decreases and attains a value of approximately 1° at 60 knots. (well below the optimum trim angle) The calculation method (Savitsky, 1964) will also show that the wetted keel length will exceed the LOA of this hull at 60 knots.—this will cause some bow penetration into the oncoming fluid and hence result in an added form resistance. This is an undesirable operating condition. To avoid bow wetting the wetted keel length should be less than approximately 0.90 LWL. The calculation method (Savitsky, 1964) indicates that this will occur at a speed of 40 knots. At this speed the trim angle is 2°—unfortunately, as shown on Fig. 1 this is substantially less than the optimum trim angle of approximately 4°.

Resistance/Displacement Ratio Variation with Speed

As shown on Fig. 2 the resistance/displacement ratio increases rapidly with increasing speed and the associated decrease in trim. At 20 knots, $R_T/\Delta = 0.10$ —a most acceptable value. At 40 knots, $R_T/\Delta = 0.20$ —an unavoidable value that may have to be accepted by default. At 60 knots, $R_T/\Delta = 0.35$ —a completely unacceptably value.

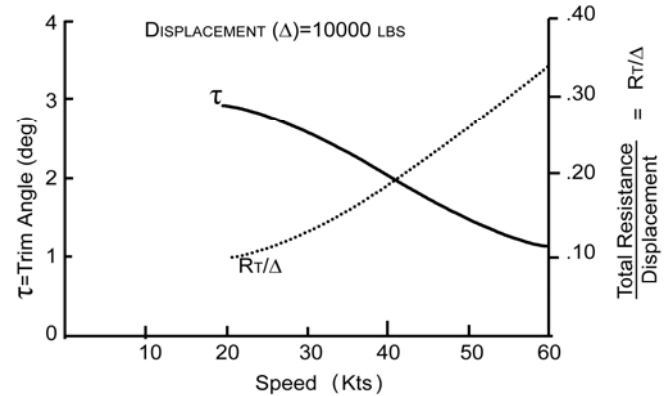
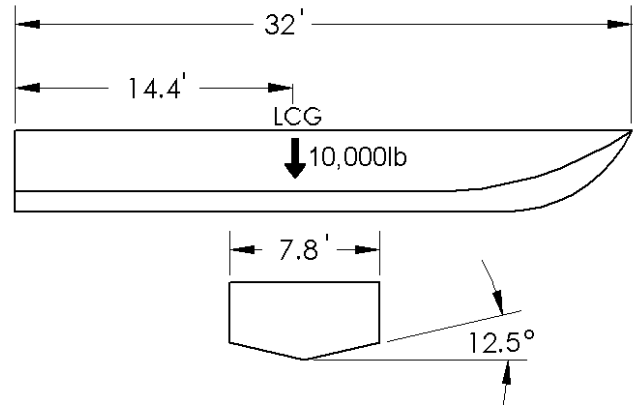


Fig. 2 Calculated Typical Trim R_T/Δ and vs. Speed - Monohull

Summary

Since the equilibrium trim angle of planing monohulls naturally decrease with increasing speed, they quickly attain values that are well below the optimum trim angle required for minimum resistance. This may be partially alleviated by designing with a further aft located LCG or incorporating some “rocker” at the transom. If these are not feasible or totally effective, an alternative option is the use of a stepped planing hull that will allow for high speed operation at a more optimum trim angle. The next section discusses the geometric features and resistance characteristics of the stepped hull and the importance of providing forebody surface wake profiles for proper total design of these hulls.

STEPPED PLANING HULLS DESIGNED TO ACHIEVE MAXIMUM LIFT/DRAG RATIO AT HIGH SPEED

This brief discussion is not intended to provide a detailed design procedure for stepped hulls. It merely presents an overview of the hydrodynamic influences that must be considered when designing these hulls for minimum hydrodynamic resistance at high speed. This may be in contrast with the multi-step racing hulls that are designed for maximum

speed and stability. It is expected that at some future date the performance of these multi-step racing stepped hulls will be better understood and their hydrodynamic lift/drag ratios documented.

The previous discussions have shown that the high speed planing monohull has relatively large hydrodynamic resistance due to its inherent characteristic of running at trim angles well below the optimum trim angle required for minimum resistance at high planing speeds. The stepped hull overcomes this deficiency in the following manner:

The hull is split transversally at a position somewhat aft of mid ship creating a forebody and afterbody. The afterbody keel is slightly raised above the forebody keel creating a “step” in the profile view (see Fig.3) hence the name “stepped hull”. In addition, the keel of the afterbody may be oriented at an appropriate angle relative to forebody keel to achieve a desired intersection with the forebody wake. The water flow from the forebody separates from the bottom at the step location and clears most of the afterbody bottom. The contour of this forebody wake governs the step height and angle of the afterbody. It is this forebody wake shape that is the primary subject of this report.

Typically approximately 90% of the total weight of a stepped hull is supported by the forebody since its lift/drag ratio is designed to be as large as possible. The remainder of the weight is supported by the afterbody or a stern appendage that penetrates the forebody wake. This appendage can be made adjustable to control the trim angle as speed is varied. It should also provide pitch damping to avoid porpoising. The LCG position is in the forebody region and slightly forward of the step. This limits the extent of the planing area on the forebody. Thus, to support 90% of the total load on a relatively small bottom area, the trim angle of the forebody must be larger than that of a monohull which uses both the forebody and afterbody planing areas. This is the key to attractiveness of the stepped hull—at high speed it can be designed to operate at the trim angle for minimum hydrodynamic resistance. To further increase the lift/drag ratio of the forebody, its trailing edge (at the step) can either be cambered longitudinally (Clement and Koelbel, 1992) or fitted with an adjustable angle trailing edge flap. The effectiveness of this later modification is discussed below.

Estimate of the Performance of a Stepped Hull

To illustrate the advantage of a stepped planing hull at high speed, the monohull shown in Fig. 1 is reconfigured into an equivalent stepped hull as shown in Fig. 3. The total displacement, 10,000 lbs (4546 kg), the LOA, 32 ft (9.8 m), the chine beam, 7.8 ft (2.4 m) and deadrise angle, 12.5°, remain the same. The afterbody length is taken to be 13.5 ft (4.1 m). The forebody load (Δ_f) is $0.90 \times 10,000 = 9,000$ lbs (4091 kg). It is assumed that the remaining 1,000 lbs (455 kg) is carried by the afterbody or a submerged or surface piercing hydrofoil that is attached to the transom and penetrates the forebody wake.

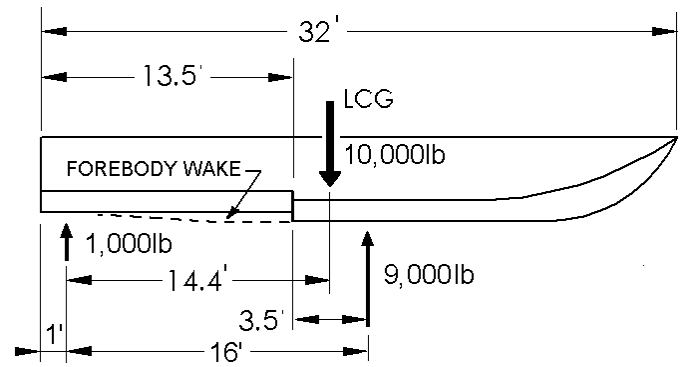


Fig. 3 Dimensions of Equivalent Stepped Hull
 $B = 7.8$ ft, $\beta = 12.5^\circ$

For the purposes of this illustration, the afterbody resistance is assumed to be small compared to the forebody so the calculated results will be for the forebody which supports a load of 9,000 lbs (4091 kg). The afterbody load is taken to be located approximately 1 ft (0.3 m) forward of the transom—this will be demonstrated in the illustrative example provided in a latter section of this paper. For pitch equilibrium the longitudinal location (L_o) of the 9,000 lb (4091 kg) load on the forebody relative to the load on the afterbody is obtained by taking moments about the resultant afterbody load location. Thus:

$$10,000 \times 14.4 = 9,000 \times L_o$$

$$\text{Thus: } L_o = 16 \text{ ft (4.9 m)}$$

Hence, the center of pressure of the 9,000 lb (4091 kg) load is $16.0 - 12.5 = 3.5$ ft (1.1 m) forward of the step. This is an important dimension in the design of the stepped hull since the stagnation line on the forebody should intersect the chine ahead of the step. Given the 9,000 lbs (4091 kg) acting 3.5 ft (1.1 m) forward of the step, the simplified format equations in Savitsky (1964) can be used to calculate the orientation of the stagnation line relative to the keel and also the keel and chine wetted lengths relative to the step. If the stagnation line intersects the step, the heavy main spray, that originates at that point will impinge upon the bottom of the afterbody and result in a substantial increase in resistance.

Performance Without Flaps Using the performance estimating equations for the forebody without flaps (Savitsky, 1964) the calculated equilibrium trim angle and resistance/displacement ratio are plotted on Fig. 4. (solid symbols) and are compared with the monohull results (curves). A transverse step was used in this illustration since it was shown in Savitsky and Brown (1976) that while a reentrant vee-transom, such as suggested by Clement and Koelbel (1992), can attain higher aspect ratios, the lift-drag ratio of the reentrant step is somewhat smaller than that of a transverse step that has the same wetted area.

The calculations for the stepped hull are limited to speeds less than 40 knots ($F_V=5.2$) and greater than 30 knots ($F_V=3.9$). At speeds greater than 40 knots, the trim angle will decrease and the stagnation line will cross the step. The main spray will thus impinge on the afterbody bottom with an un-quantified associated increase in resistance. This is an undesirable operating condition, however it can be alleviated by an adjustable hydrofoil attached to the stern than will control the trim. At speeds less than 30 knots, the flow from the forebody may not completely ventilate at the step. This will result in an increased form drag of the forebody which, at the present time, cannot be easily calculated. It is likely that, at speeds less than 30 knots, the resistance of the stepped hull will be greater than that of the equivalent monohull.

From Fig. 4 it is seen that the running trim angles of the stepped hull are larger than those of the monohull and well within the favorable range of trim angles as shown on Fig. 1. At an operating speed of 40 knots, the trim angle is 4.3° and the R_T/Δ for the stepped hull is nearly $\frac{1}{2}$ that of the monohull. This is a significant improvement in performance that justifies consideration of the stepped hull for high speed operation. At 30 knots, ($F_V=3.9$) the R_T/Δ for both hull forms are nearly equal, so that the more simply constructed monohull would be the desired hull form.

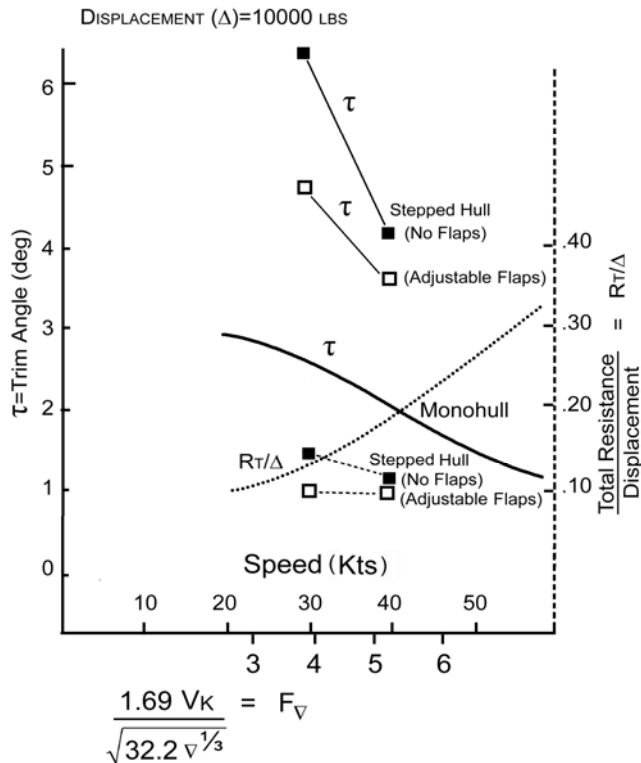


Fig. 4: Calculated Trim and R_T/Δ vs. Speed – Monohull vs. Stepped Hulls

Performance With Controlled Forebody Transom Flaps

Clement and Koelbel (1992) recommended that the after bottom of the forebody have longitudinal camber that is defined by a Johnson 3 term profile (Johnson, 1961).

Since the primary curvature of the cambered section is along a small area just forward of the trailing edge, it was speculated that a deflected flap located at the trailing edge of the forebody may have similar beneficial effects on improving the lift/drag ratio. Studies of the effectiveness of transom flaps installed on planing craft are reported in Savitsky and Brown (1976). It was shown that for a fixed trim, load and speed the drag/lift ratio was reduced as the deflected flap area was increased. Savitsky and Brown (1976) also presents methods for calculating the flap effectiveness on a planing craft. Using these methods, a flap was selected for the stepped hull just described. The dimensions and deflection of the flap which was attached to the hull bottom were:

- Full span = 7.8 ft (2.4 m)
- Chord = 0.40 ft (0.12 m)
- Deflection: 2.5° @ 40 knots
- 10.0° @ 30 knots

The flap deflection angles were selected to assure that the stagnation line on the forebody intersected the chine at each test speed.

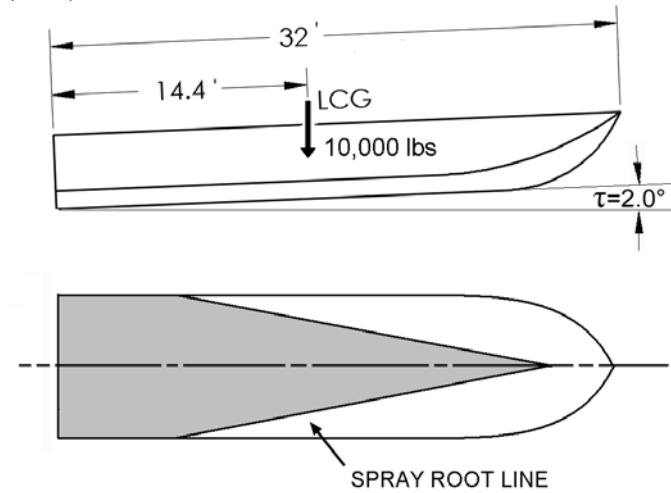
It is important to understand that the objective of this brief introduction to stepped planing hulls is not to compare the performance of a transverse step with the re-entrant and longitudinally cambered step described by Clement and Koelbel. Each has their advantages and disadvantages. Rather, since the primary objective of this study is to supply wake data, the transverse step was used as a simple illustration to emphasize the need for such data when designing stepped hulls.

Using the methods of Savitsky (1964) and Savitsky and Brown (1976), the equilibrium trim angles and R_T/Δ values were calculated and are presented on Fig. 4. As expected, the flap reduced the running trim and, in addition, reduced R_T/Δ at 30 and 40 knots. At these speeds, the R_T/Δ was 0.10, a most significant improvement compared to the planing monohull. It is important to note that, while the deflected flap reduced the trim angle at 40 knots, this lower trim angle was still within the acceptable trim range as shown on Fig. 1. It is suggested that a stepped planing hull may be designed without active trim control if the LCG is located so that the craft operates at optimum trim at the design high speed. For modest changes in trim, due to changes in speed, the R_T/Δ varies very little.

Comparison of Wetted Areas and Performance of a Stepped Hull vs. a Monohull

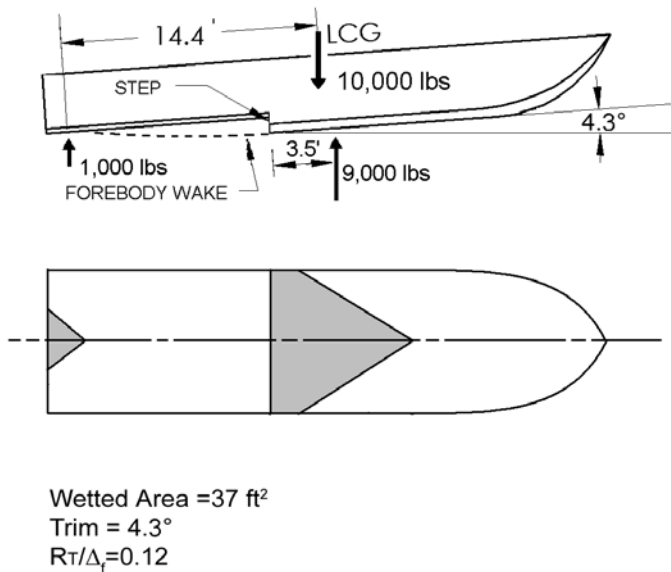
Figures 5(a-c) present this comparison for a 40 knot planing speed. The results are self explanatory. Note that the afterbody

forces are not considered. Although not discussed in this paper it is likely that, without an afterbody contribution to lift and especially pitch damping, the forebody will porpoise. This can be demonstrated by comparing the tabulated equilibrium trim angles with the porpoising limit criteria given in Savitsky (1964).



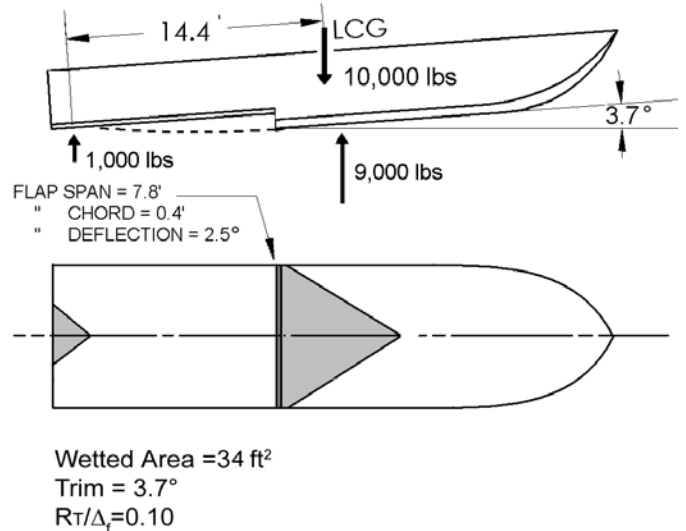
Wetted Area = 164 ft²
 Trim = 2.0°
 $R\tau/\Delta_V = 0.20$

Fig. 5(a) Comparison of Trim and Wetted Areas Monohull
 ($\Delta = 10,000$ lb; $V_K = 40$; $F_V = 5.1$)



Wetted Area = 37 ft²
 Trim = 4.3°
 $R\tau/\Delta_V = 0.12$

Fig. 5(b) Comparison of Trim and Wetted Areas Stepped Hull
 ($\Delta = 0.9 \times 10,000 = 9,000$ lb; $V_K = 40$; $F_V = 5.1$)



Wetted Area = 34 ft²
 Trim = 3.7°
 $R\tau/\Delta_V = 0.10$

Fig. 5(c) Comparison of Trim and Wetted Areas Stepped Hull With Flap on Transom of Forebody
 (Forebody Load = 9,000 lb; $V_K = 40$; $F_V = 5.2$)

Summary

The stepped planing hull configuration offers significant reductions in total resistance at F_V greater than approximately 5.0 as compared to a similar planing monohull.

Unfortunately, there has been a dearth of data on the shape of the forebody wake which interacts with the afterbody. This inhibits the complete development of an analytical prediction method. The subsequent section of this paper presents such data.

SURFACE WAVE CONTOURS IN THE WAKE OF PLANING SURFACES

Previous Experimental Studies

For the reader who may not be familiar with the geometric form of the surface wake aft of a planing craft, Fig. 6, taken from Korvin-Kroukovsky, Savitsky and Lehman (1948b), presents a sketch of typical transverse and longitudinal wave contours aft of a 10° deadrise hull that has a ventilated transom. As shown, the defined surface geometry extends 6 beams aft of the transom and 3 beams on either side of the longitudinal centerline. Two characteristic geometric features are immediately apparent. Along the aft extension of the longitudinal centerline of the hull, the separated flow from the transom is initially deflected below the level waterline. As the distance aft of the transom increases, this depressed flow slowly rises and crosses the level surface to form the familiar "rooster tail" associated with planing craft. The second readily visible geometric features are the two longitudinally directed wave crests that are initiated at the chines. Their transverse distance from the centerline increases with distance aft of the

transom. Further, these crests maintain a nearly constant height for a distance of approximately 6 beams aft of the transom. Korvin-Kroukovsky, Savitsky and Lehman (1948a, 1948b, 1949) contain many such plots for a range of planing conditions (trim angle, loading, and speed coefficients)

appropriate to seaplane hulls. Specifically, the summary report of these three references (Korvin-Kroukovsky, Savitsky and Lehman, 1949) questions the reliability of these data at trim angles less than 6° . This is precisely the trim range appropriate to stepped planing hulls.

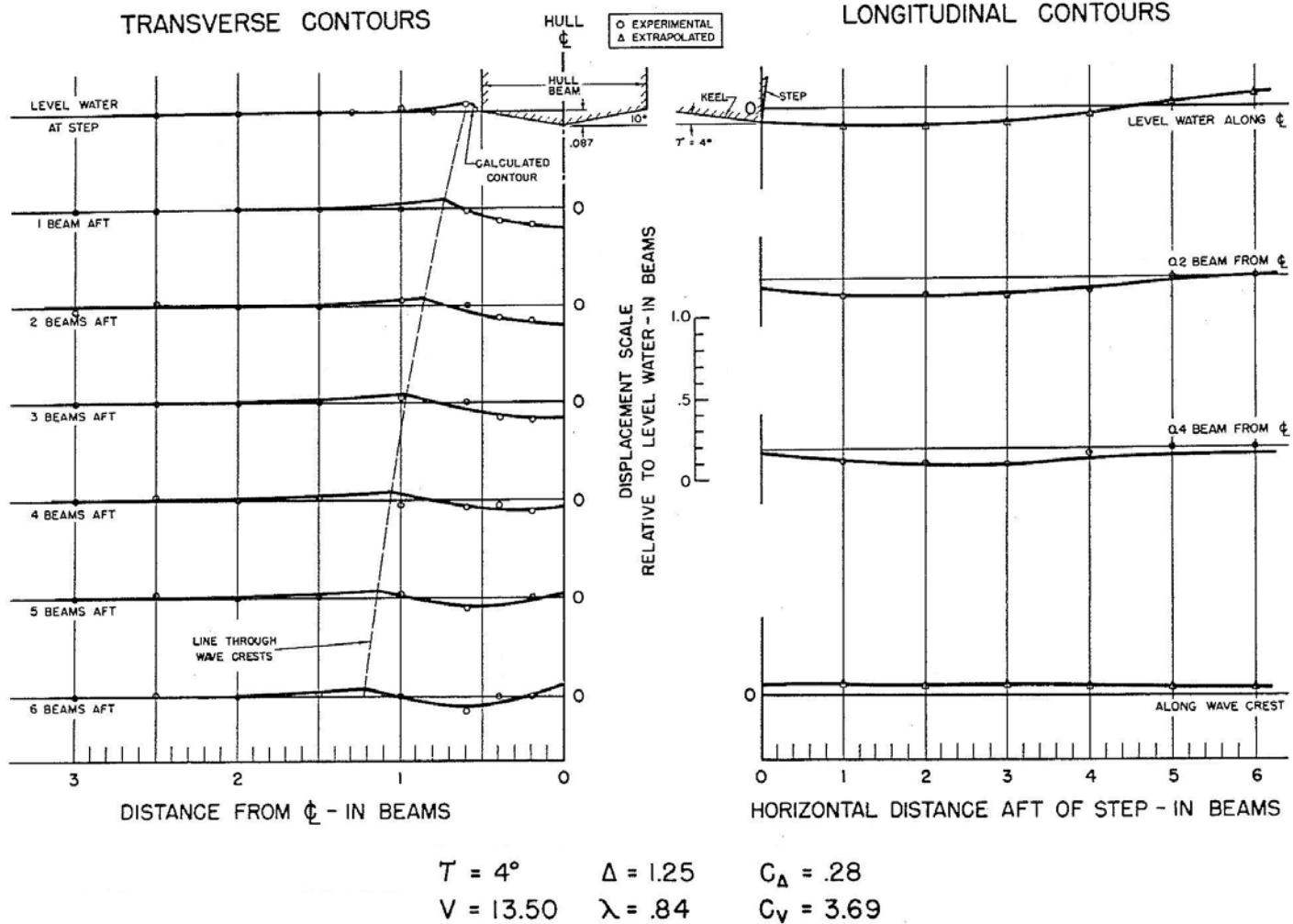


Fig. 6 Experimentally Obtained Surface Wave Contours Aft of Transom of 10 Degree Deadrise Hull (Korvin-Kroukovsky, Savitsky and Lehman, 1948b)

The wake data presented in Van Dyck (1960) are mainly applicable to seaplanes using hydro skis as landing and take off devices. For that application, the test loading, speed, and trim conditions are substantially out of range with those associated with stepped planing hulls. Of particular significance in that study however was the observation that the flow in any transverse section aft of the transom is essentially two-dimensional. That is, the trough developed by the hull fills in from the sides and bottom. Hence the time history of the surface oscillation in the transverse plane can be combined with the forward speed to develop the longitudinal profiles of the surface wake. It was also shown, that for a given depth of keel and downwash velocity ($V \sin \tau$), the resultant wake shape remains the same regardless of the separate values of V and τ .

One of the earliest publications on wake shapes was a paper by Sottorf, a German scientist who, in 1932, conducted model tests related to water-based aircraft. His work, which was subsequently translated by NACA, (Sottorf, 1934) presents several examples of the longitudinal centerline profile of the wake. Unfortunately, his test conditions were limited to one speed and one displacement for several deadrise hulls and hence are insufficient for the general design of stepped planing craft.

The original intent of the present study was to extract wake data from these references that would be suitable for the stepped planing hulls. It soon became apparent that most of the published data would not be applicable. Hence, a model test program was undertaken to provide wake data for planing conditions appropriate to the stepped hull. A subsequent section

of this report describes this test program and presents the results in a format that can be directly used by the naval architect to define the step height and afterbody angle to properly orient the afterbody relative to the forebody wake. An example of this design procedure is also included in the present report.

Analytical Efforts to Define Surface Wake Geometry

MacPhail and Tye In 1944, MacPhail and Tye of the Royal Aircraft Establishment, Farnborough, England published a theoretical analysis of the wake geometry of planing hulls (MacPhail and Tye, 1944). The motivation for this study was “high speed porpoising of flying boat models seem to be seriously aggravated by inopportune striking of the rear step on the surface of the through behind the main step. It would clearly be useful to know the shape of the trough in order to predict the likelihood of such an occurrence”

In their analysis, the authors examine a planing surface having a fixed trim angle and constant forward speed passing through a transverse plane that is fixed in space and normal to the level water surface. At planing speeds the flow separates from the bottom of the hull and the transom and is completely ventilated to the atmosphere. At the instant of passage of the transom through this plane, a trough conforming to the shape of the hull bottom and having a slight local “wave rise “ just outboard of the chines appears. This trough has imposed on it a vertical velocity equal to the planing velocity times the sine of the trim angle. It is further assumed that the trough fills in from the sides and bottom under the influence of gravity and that the entire process is two dimensional in transverse planes. This assumption was essentially confirmed by model tests reported by Van Dyck (1960). Using potential flow theory the authors compute the time history of the vertical position of the free-surface as the trough fills in. Multiplying time by the forward velocity of the hull translates into a longitudinal position aft of the transom. Thus the longitudinal profile of the wake can be defined.

MacPhail and Tye compare their analytical results with the limited amount of model data that was available in 1944. They conclude that, even with the introduction of empirical factors into the analytical model that are required to obtain a reasonable agreement with the overall geometric features, there is still further development required for a reliable quantitative prediction of the wake shape. They suggest possible additions to their analytical approach that are expected to improve the accuracy of their method. Interested readers are encouraged to study this reference. The authors did not further pursue this study because of the pressure of more urgent problems during World War 2.

Shoemaker Zero Deadrise Wake Profile In 1934 J.M. Shoemaker published an analytical method for calculating the wake behind a flat plate planing at a fixed trim angle (Shoemaker, 1934). He assumed that the wake shape cross-section was essentially a rectangular trough. Neglecting static lift, and using the principle of conservation of energy, he calculated the height of the wake profile aft of the plate. These results compared favorably with data collected by Sottorf (1934) in tests of a flat plate.

Computational Fluid Dynamics (CFD) Computational Fluid Dynamics methods can be a useful tool for predicting the surface wake profiles behind a planing hull. There are many commercially available codes that may be applied. As with all CFD developments, to assure accurate results, it is essential to select a mesh density that is appropriate to the complexity of the geometry of the body. This usually requires experimental data to guide the iterative process of selecting the proper mesh size and to also judge the reality of the final analytical predictions. The present report provides experimental data that can be used by researchers interested in developing a CFD solution for the planing hull wake geometry.

It is believed that, even if CFD software becomes available, it will not be at the level where it can be easily used by small craft designers who may have a limited basic knowledge of the underlying numerics. Consequently, the present study provides a wide base of experimental data which are presented in a format that is directly and easily used by the designer of stepped planing hulls. These data will also be quite useful to potential CFD analysts who may be interested in this problem. The authors encourage the development of CFD since such a tool may be useful in extending the range of parametric variables at modest cost.

Present Experimental Studies

Scope of Model Tests The wake region surveyed in this test program was limited to the surface area located $\frac{1}{2}$ beam on either side of the aft extended longitudinal centerline, and 3 beams aft of the transom of the test models. This is in contrast to the large surface area shown on Fig. 6. The smaller area is justified because the length of afterbodies are typically between 2 and 3 beams so that the collected data are well within the practical design range for stepped hulls. This limited range of study reduced the number of test runs and hence expedited the completion of this study.

Test Models The test models were 9 inch beam, 10°, 20°, and 30° prismatic hulls. They were constructed of white pine and the chines and transom were sharpened to assure complete flow separation from these edges. Fig. 7 shows the lines of the 20° deadrise parent model.

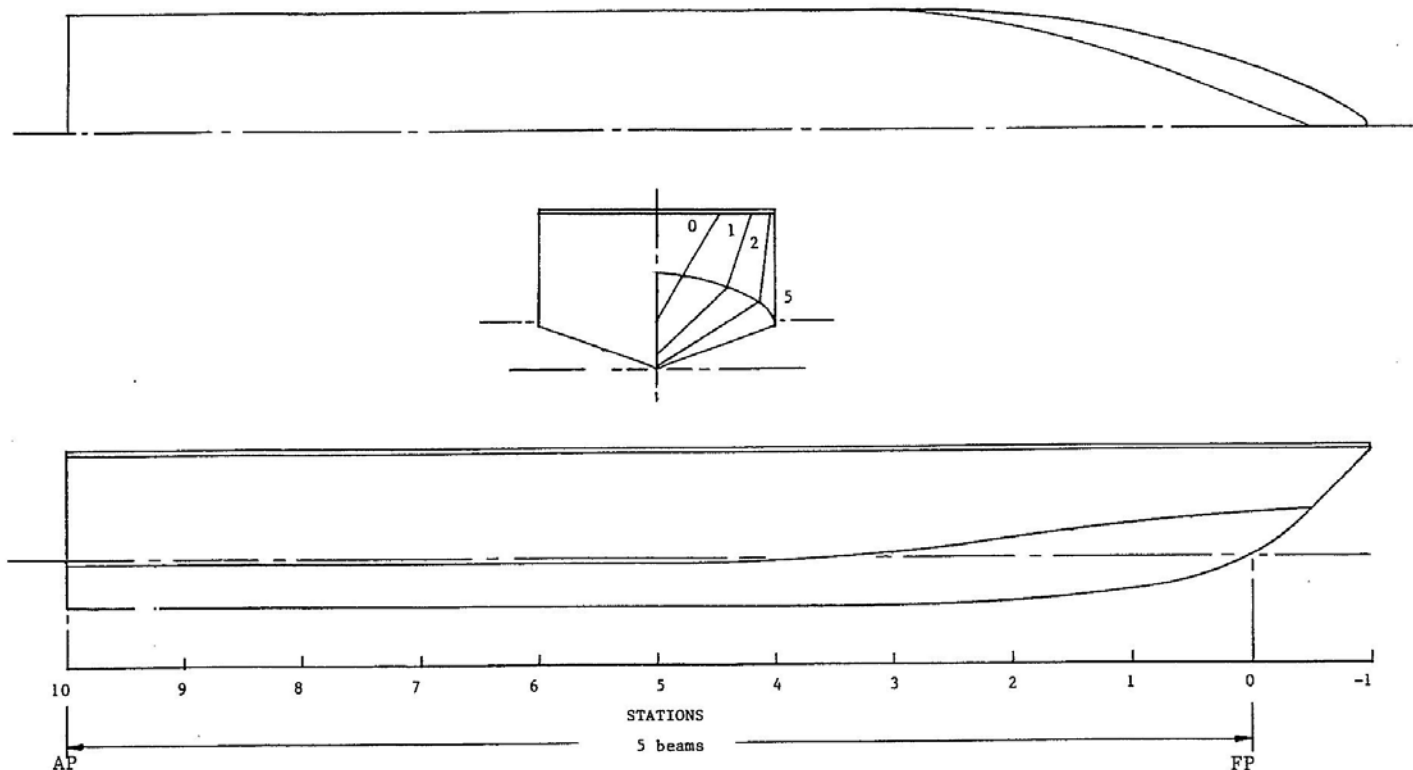


Fig. 7 Lines of 20 Degree, 9" Beam Parent Model

Measurement of Surface Wake Contours Several methods for measuring the wake contours were considered. These included overhead stereo photography; a traversing sonic probe mounted above the water surface; and a system of vertical probes that could be adjusted vertically until they just touched the water surface. It was concluded that the simplest method was to attach a thin vertical plate, marked with a grid, to the transom of the model. The bottom of the plate was aligned with the bottom of the model at the transom. It extended 3 beams aft of the transom (see photographs in Fig. 8). The longitudinal wake profile was readily identified against this grid.

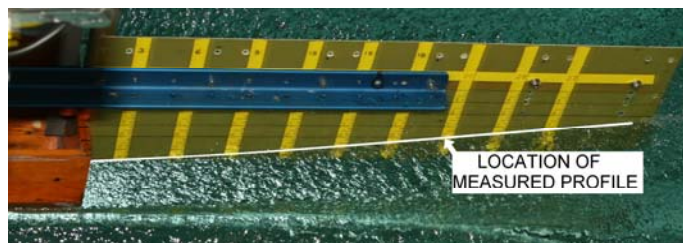


Fig. 8(b) Typical Wake Profile Looking into Trough from Camera on Ceiling



Fig. 8(a) Typical Stern Quartering View From Camera on Tank Sill

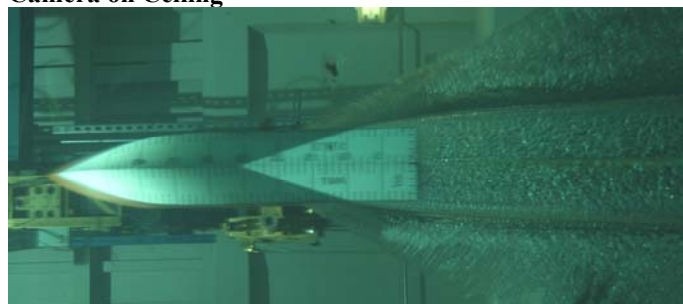
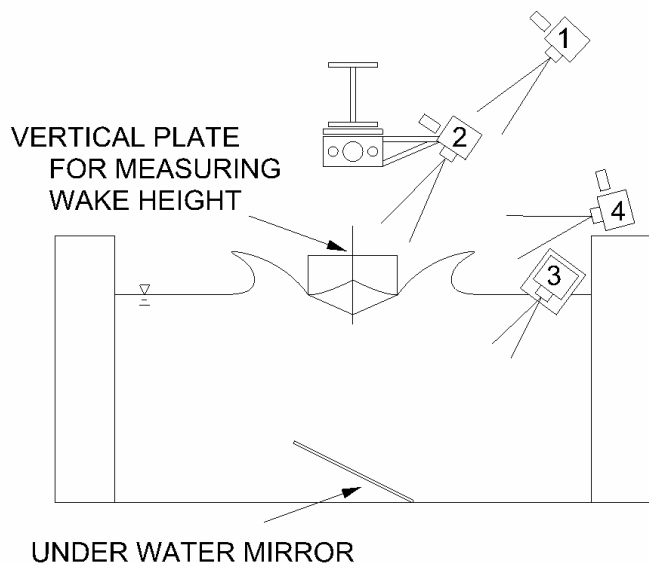


Fig. 8(c) Typical Under Water Photo Showing Wetted Lengths



- (1) CAMERA ON CEILING
-AND-
(2) CAMERA ON TOWING CARRIAGE
FOR PHOTOS INTO TROUGH
(WAKE PROFILES MEASURED
WITH THESE CAMERAS)
- (3) CAMERA IN WATER RESISTANT BOX
FOR WETTED LENGTHS
- (4) CAMERA ON TANK SILL
FOR HEIGHT OF SPRAY

Fig. 9 Cross Section of Towing Tank Showing Camera Locations Used During Tests

As shown on the sketch in Fig. 9, four cameras were used to record the test results. One camera was mounted on the ceiling of the tank and provided a view directly into the wake through. A second camera was mounted high on the moving test carriage and also provided a view directly into the wake trough. Wake profiles were recorded by both these cameras. A third camera was mounted on the tank sill and provided data on the spray height. The fourth camera was located in a water tight box and provided underwater photographs of the wetted bottom area of the model. The camera on the test carriage photographed the grid 4 times during each run. Photographs were taken of the longitudinal wake contours along the extended hull centerline; $\frac{1}{4}$ beam from the centerline; and along the chine.

The underwater photographs provided the wetted keel and chine lengths. When combined with the trim angle, a measure of the keel draft at the transom was obtained.

Range of Model Test Conditions A test matrix was developed for a range of loading, wetted lengths, and speeds that were considered to be representative of stepped hull designs and their operating conditions.

Load Coefficient = $C_{\Delta} = \Delta/wB^3$: After a review of the dimensions and displacements of many planing hulls it appeared that loading coefficients varied between 0.40 and 0.80. The smaller values are more nearly representative of recreational craft while the tendency to larger values is usually associated with heavily loaded military craft. Of course, it is the designers' decision to specify the loading on the craft. These observations were used primarily to select a range of test loadings that would be realistic and also result in a reasonably sized test matrix. Thus, the test loading coefficients were:

$$C_{\Delta} = 0.40, 0.60, \text{ and } 0.80$$

Trim Angle (τ) Range: The previous discussions of the operating conditions of the stepped hull concluded that its favorable resistance characteristics are a result of running at optimum trim angles as shown on Fig.1. It is seen that resistance/weight ratio is at its minimum with only a small variation for trim angles between 3° and 5° . The test range of trim angles were somewhat extended to include a trim angle of 2° . Thus:

$$\tau = 2, 3, 4, 5^{\circ}$$

Speed Coefficient = $C_v = V/\sqrt{gB}$ It was previously stated that the advantages of a stepped hull are primarily at high speed where the equivalent monohull is likely running at unfavorably small trim angles. It was also suggested the stepped hull is best used at volume Froude numbers greater than 5.0. Using the definition of speed coefficient, C_v , that is more commonly used by planing hull hydrodynamic researchers, it appears that a $C_v = 4$ may represent a lower limit of speed for the stepped hull. Hence, the test values of C_v were selected to be:

$$C_v = 4, 6, 8$$

Test Procedure: The models were fixed in trim and were free to heave. The sequence of tests runs was as follows:

For each deadrise hull the model was fixed at specified trim angle and loaded to correspond to a prescribed value of C_{Δ} . Tests were then conducted over a speed range corresponding to the range of C_v values identified above. For the centerline and quarter buttock of the 20° hull, the surface wave profile relative to the lower edge of the grid was photographed four times during the length of the run. The heights of the wave were measured at 9 evenly spaced ($\frac{1}{3}$ beam) intervals aft of the transom. For the 10° and 20° hulls, data were obtained at 3 evenly spaced (1.0 beams) intervals aft of the transom. The results from the different photographs were combined arithmetically to obtain average values. In addition, an underwater photograph of the wetted area was taken to identify the wetted keel and chine lengths. For those tests conditions where the stagnation line crossed the transom (chines dry condition) the wetted width of the transom was also photographed. This procedure was repeated for each of the deadrise models over the same range of trim angles, C_{Δ} , and C_v

identified above. There were nearly 2,500 data points collected during what was planned to be a limited test program to define the surface wake profile over a relatively small area of the wake. It would be impractical to tabulate these data in the present report. They are in storage at the Davidson Laboratory and can be made available to interested researchers.

Presentation of Test Results

Although the number of experimental data points appear to be overwhelming, it was found that the longitudinal wake profiles could be presented simply in a graphical form easily used by stepped hull designers. The sketches of Fig. 10 are diagrams of the reference axis used to identify the surface wake profiles. Figures 11, 12, and 13 present these results for hull deadrise angles of 10°, 20° and 30° respectively. Each figure presents the longitudinal centerline wake profile on the left and the corresponding ¼ buttock line wake profile on the right. Each contain three vertically arranged plots that provide results for L_k/B values that assure chines wet operating conditions and these are a function of trim and deadrise angle. Fig. 14 presents a tabulation of the minimum values of L_k/B . These values were developed using an assumed minimum value of 0.10B for minimum L_c and the quantity $(L_k - L_c)$ as given in Savitsky (1964).

Within each plot the ordinate is the wake height in beams (relative to the bottom edge of the grid) and the abscissa is the distance aft of the transom in beams. Note that the vertical scale is 4 times the horizontal scale so that the actual slopes of the wake contours are exaggerated. The curves themselves are for combinations of trim angle = 3° and 5° and $C_v = 4$ and 8. Although similar curves are available for a trim angle of 4° and C_v of 6.0, they were not included on these figures since they would crowd the plots and make it somewhat more cumbersome to use. For trim = 4° and $C_v = 6.0$ the designer can easily interpolate between the plotted curves.

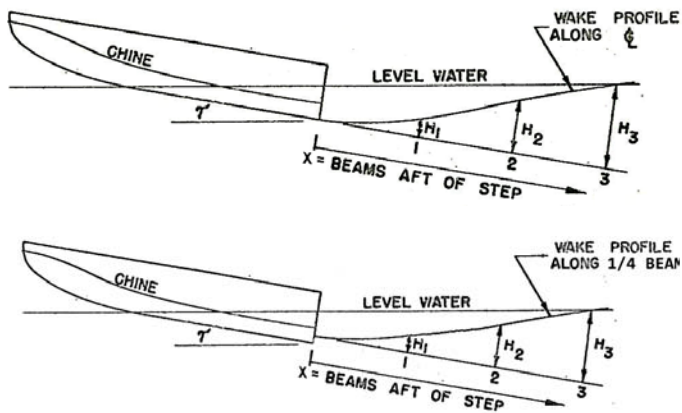


Fig. 10 Diagram of Reference Axis for Wake Profile Equations (Top) Centerline Profile (Bottom) Quarter Beam Profile

Development of Surface Wake Profiles on Figures 11,12 and 13 While the wake profiles are shown to plot smoothly and to vary systematically as the operational parameters are varied, the data itself had scatter (+/- .03 beams), and anomalies. As is usual in analyzing large data collections, a fairing procedure was developed to provide faired curves through the data. Rather than use computer based methods to arbitrarily fair the data, it was decided to develop empirical equations that are based upon physical phenomena that can be associated with the development of the wake. Specifically, the following physical phenomena were to be represented in the empirical equations.

- 1) The depth of the keel at the transom relative to the level water-line. For a given deadrise this defines the initial cavity just behind the planing surface. This depth is equal to $L_k \sin \tau$. For the relatively small trim angles associated with minimum lift/drag ratios, this can be written as $L_k \tau / 57.3$.
- 2) The downwash velocity at the transom = f (planing velocity and trim angle). In the empirical developments, it appeared that using $\sqrt{\tau}$ best represented the data. In this case τ is in degrees.
- 3) Combining (1) and (2), it was found that the combination $(L_k \tau^{1.5} / 57.3)$ was an important parameter when collapsing the data.
- 4) The longitudinal profiles of the surface wake appear to be represented by sine curves whose origins are at the intersection of the submerged keel and the transom or the intersection of the quarter beam line and the transom.
- 5) For a given draft and trim angle the height of the wake profile at a given distance aft of the hull transom is inversely proportional to the speed coefficient C_v . This follows from the conclusions of Van Dyck (1960) where it is shown that, given fixed trim and draft, the formation of the three-dimensional wake geometry is essentially the result of two-dimensional flow in a vertical plane. It was shown that the time history of the two-dimensional flow (relative to the level water surface) was essentially the same for any combination of trim and speed as long as $V \sin \tau$ is constant. For the relatively small trim angles, shallow drafts and longitudinal positions $\leq 3B$ aft of the step that are associated with stepped planing hulls, there is only a small variation in the two dimensional time histories with $V \sin \tau$. This time history is converted to longitudinal positions along the three-dimensional wake by multiplying time by the speed of the craft. Thus: $T = X/V \approx X/ C_v$. The vertical displacement of the wake increases with time, T (at least for $X \leq 3B$). Hence, for a given X , T decreases as $1/ C_v$, so that the wake displacement decreases as a function of $1/ C_v$.

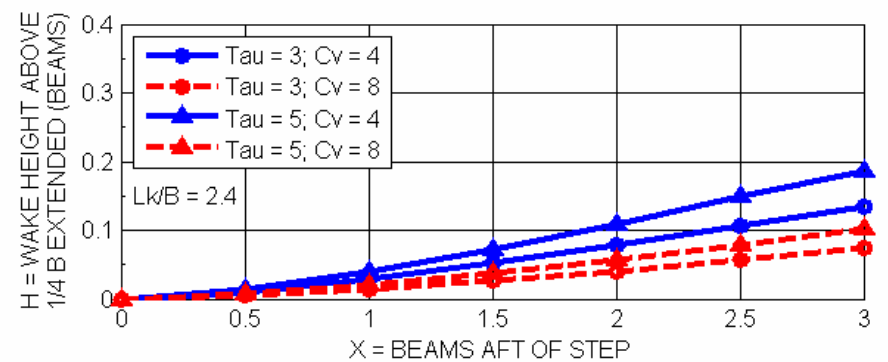
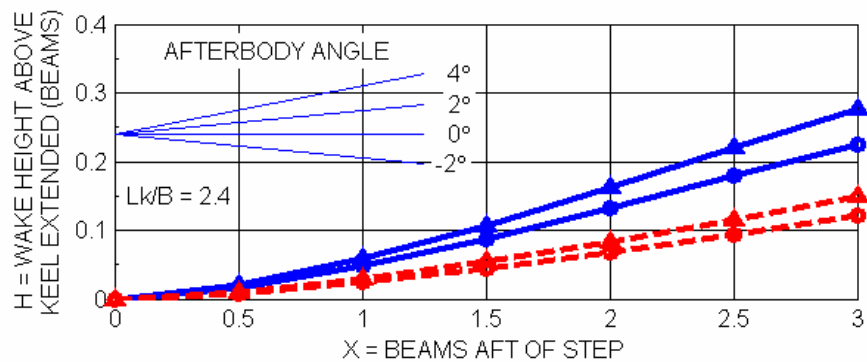
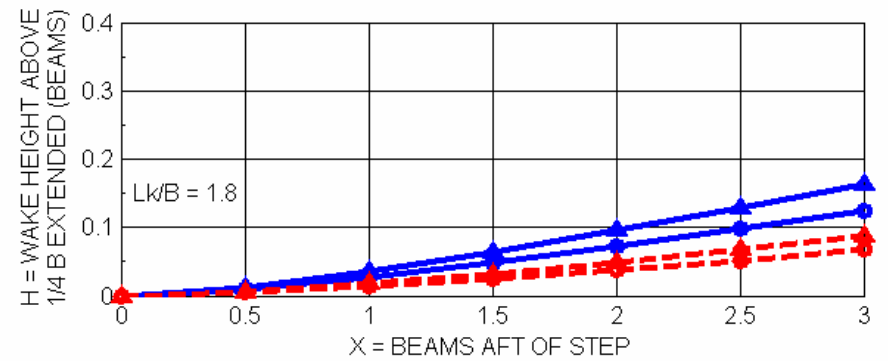
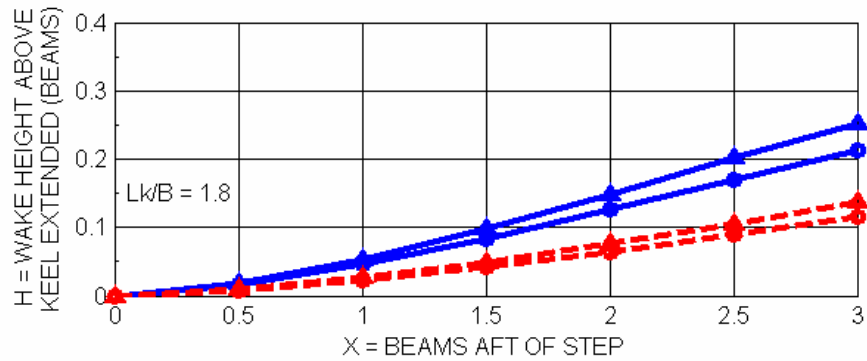
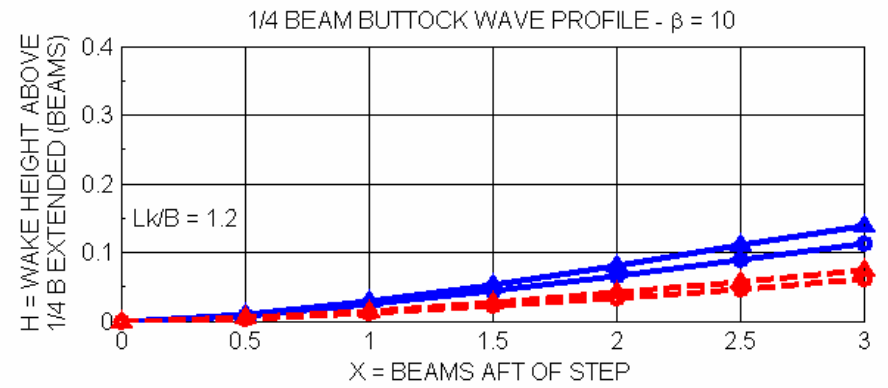
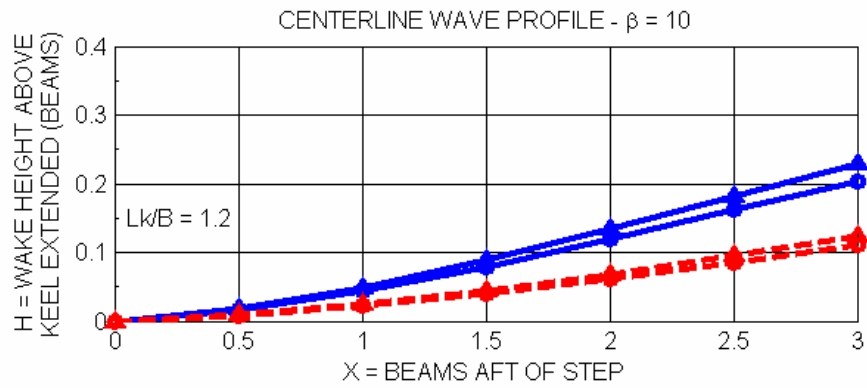


Fig. 11 Longitudinal Surface Wave Contours Along Wake of Prismatic Planing Surface $\beta = 10^\circ$

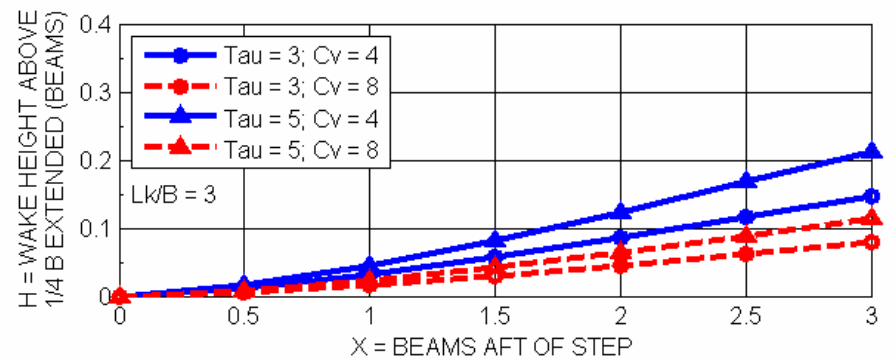
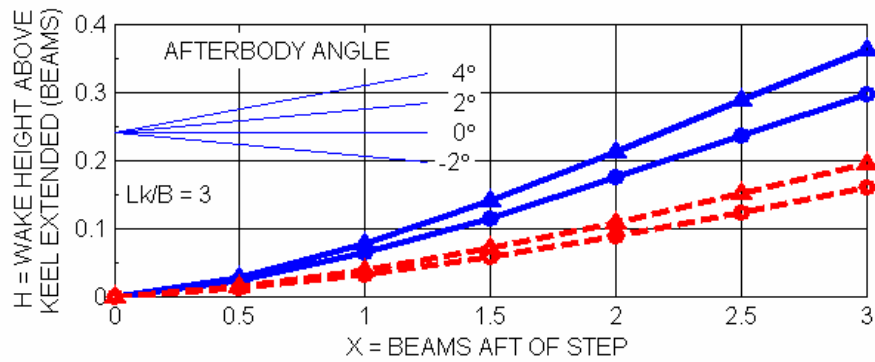
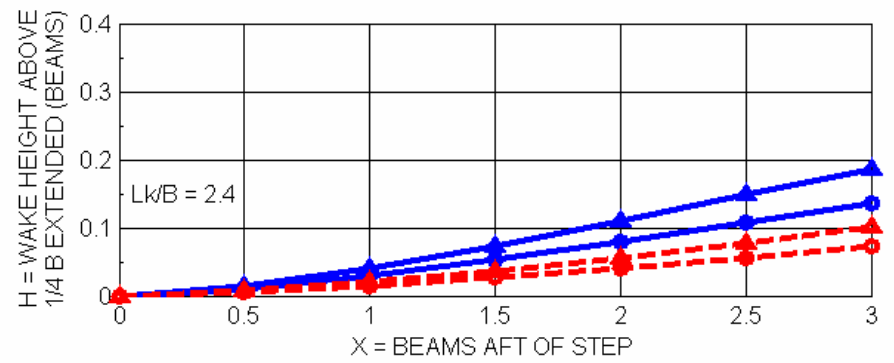
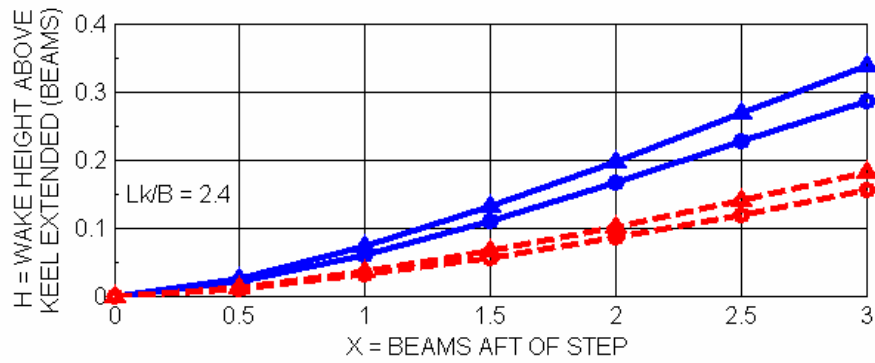
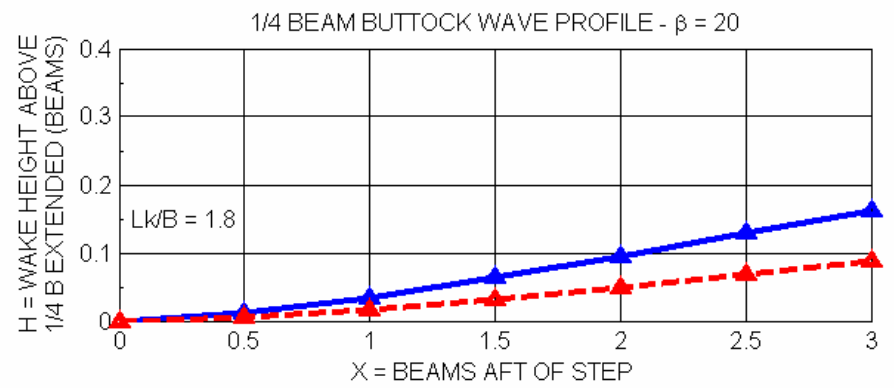
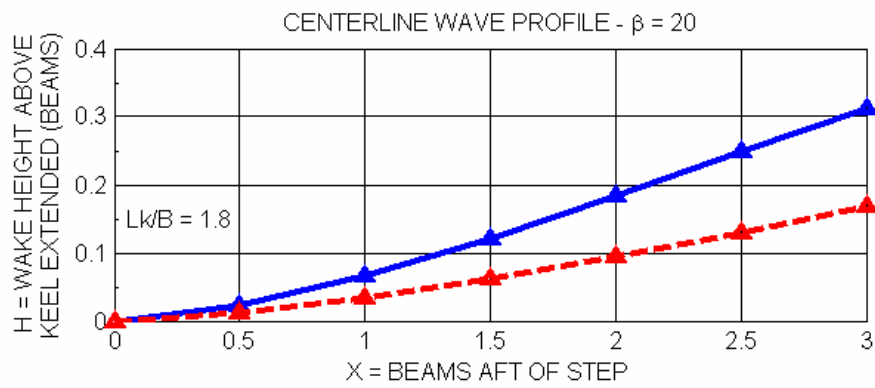


Fig. 12 Longitudinal Surface Wave Contours Along Wake of Prismatic Planing Surface $\beta = 20^\circ$

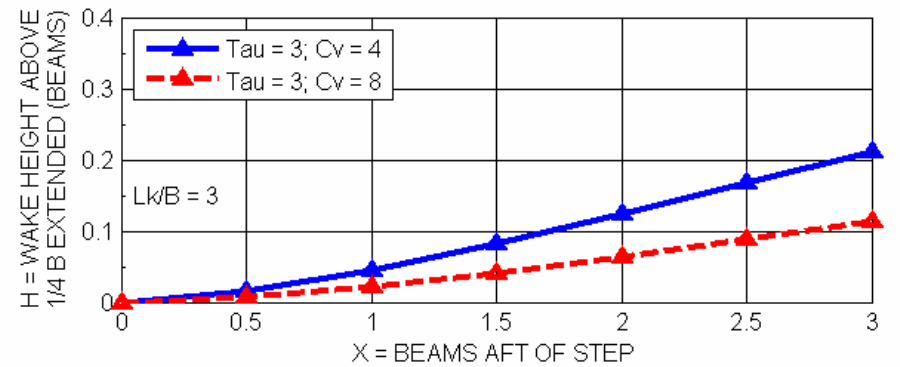
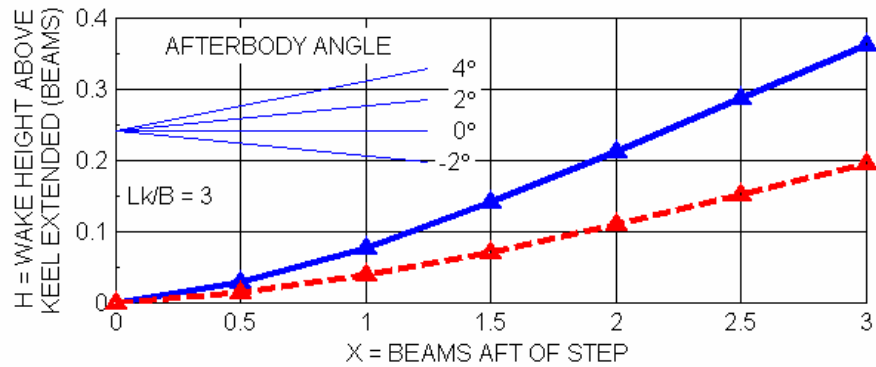
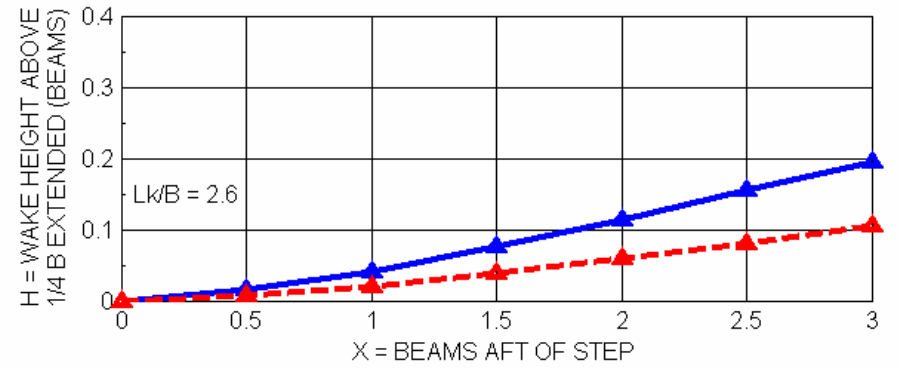
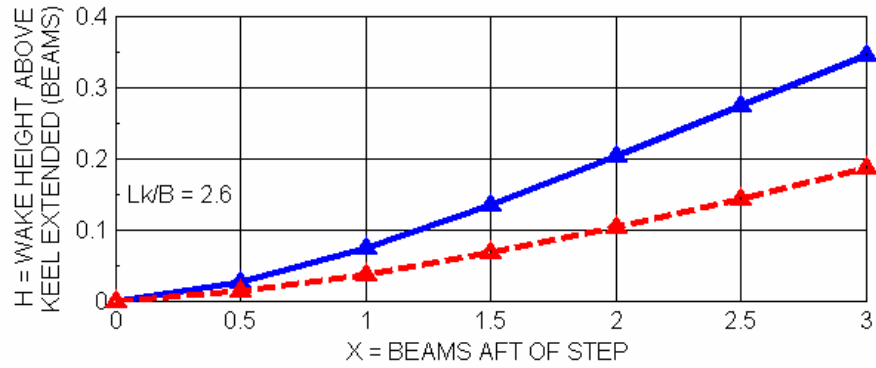
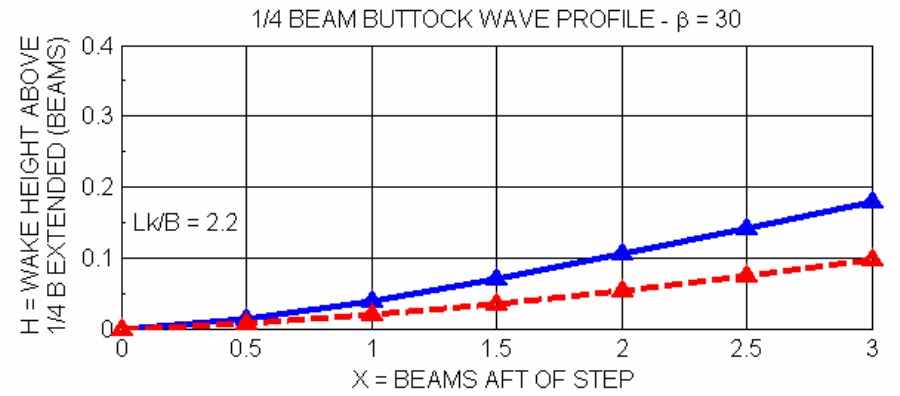
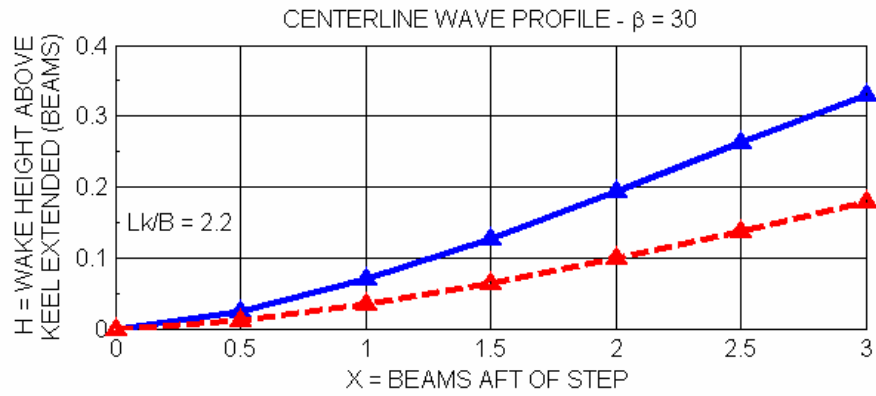


Fig. 13 Longitudinal Surface Wave Contours Along Wake of Prismatic Planing Surface $\beta = 30^\circ$

Using the above physical phenomena inputs as guidance, empirical equations were developed which best represented the experimental data. This required the selection of correlation factors which are necessary to quantify the equations and to obtain agreement with the data. The resulting formulations are summarized as shown:

Equations for Longitudinal Surface Wake Profiles

Centerline Profile:

$$\beta = 10^\circ$$

$$H = 0.17 [1.5 + 0.03 L_k \tau^{1.5}] \text{Sin} \left[\frac{\pi}{C_v} \left(\frac{X}{3} \right)^{1.5} \right] \quad (4)$$

$$\beta = 20^\circ$$

$$H = 0.17 [2.0 + 0.03 L_k \tau^{1.5}] \text{Sin} \left[\frac{\pi}{C_v} \left(\frac{X}{3} \right)^{1.5} \right] \quad (5)$$

$$\beta = 30^\circ$$

$$H = 0.17 [2.0 + 0.03 L_k \tau^{1.5}] \text{Sin} \left[\frac{\pi}{C_v} \left(\frac{X}{3} \right)^{1.5} \right] \quad (6)$$

1/4 Beam Buttock

$$\beta = 10^\circ$$

$$H = 0.17 [0.75 + 0.03 L_k \tau^{1.5}] \text{Sin} \left[\frac{\pi}{C_v} \left(\frac{X}{3} \right)^{1.5} \right] \quad (7)$$

$$\beta = 20^\circ$$

$$H = 0.17 [0.75 + 0.03 L_k \tau^{1.5}] \text{Sin} \left[\frac{\pi}{C_v} \left(\frac{X}{3} \right)^{1.5} \right] \quad (8)$$

$$\beta = 30^\circ$$

$$H = 0.17 [0.75 + 0.03 L_k \tau^{1.5}] \text{Sin} \left[\frac{\pi}{C_v} \left(\frac{X}{3} \right)^{1.5} \right] \quad (9)$$

where:

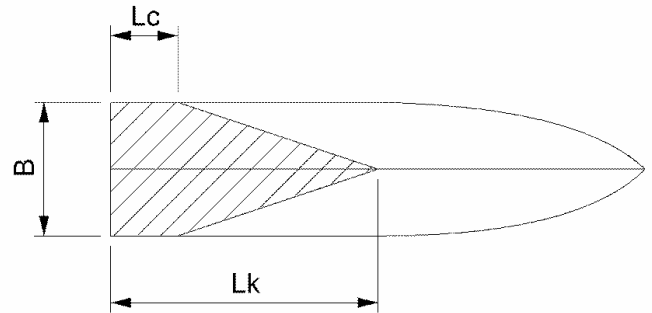
- H = height of wake profile above extended keel or 1/4 buttock, beams
- L_k = wetted keel length, beams
- τ = trim angle, degrees
- X = distance aft of transom, beams
- B = beam
- C_v = speed coefficient, V/\sqrt{gB}

Limits of Application It is essential that the application of any data based equations be limited to the range and combination of parameters used in the test program. For this study:

- $10^\circ \leq \beta \leq 30^\circ$
- $3^\circ \leq \tau \leq 5^\circ$
- $L_k \geq 0.10 + \tan \beta / \pi \tan \tau$
- $0.017 L_k \tau^{1.5} \geq 0.18$
- $L_k < 3.5B$ for 20° and 30° deadrise and $< 2.5B$ for 10°
- $4.0 \leq C_v \leq 8.0$
- $X \leq 3B$

The reason for the lower limit on L_k follows from the requirement that the stagnation line should cross the chine rather than the transom of the forebody. In fact, it is recommended that the wetted chine length be at least 0.10 beams. If the stagnation line does cross the transom (this is called the chines dry planing condition) intense aft flowing spray jets will be developed at these points. These jets will impact the afterbody of a stepped boat and result in a large drag increment and possible longitudinal instability. A subsequent section of this paper illustrates the severity of these jets.

The quantity $(L_k \tau^{1.5}/57.3) \geq 0.18$ represents the lower limit of this parameter as tested in the present study.



$$\frac{L_k}{B} = 0.10 + \frac{L_k - L_c}{B} = 0.10 + \frac{\tan \beta}{\pi \tan \tau}$$

$\frac{L_k}{B}$	$\beta = 10^\circ$	$\beta = 20^\circ$	$\beta = 30^\circ$
$\tau = 2^\circ$	1.71	3.41	5.36
$\tau = 3^\circ$	1.17	2.31	3.60
$\tau = 4^\circ$	0.90	1.76	2.72
$\tau = 5^\circ$	0.74	1.42	2.20

Fig. 14 Minimum Values of L_k/B to Avoid Chines Dry Condition

Discussion of Wake Profiles

Comparisons of the above empirical equations with the test data are shown on Fig. 15. There is good agreement between the equations and test data. The curves shown on Figures 11, 12 and 13 are developed from these equations and provide a clear graphical representation of the appearance of the forebody wakes. Note that the parameters defining the curves are varied in even increments. A designer using these figures can either interpolate between the curves for odd values of these parameters or can use the equations to obtain wake profiles for specific combinations of L_k , τ , and C_v . The equations can be easily evaluated.

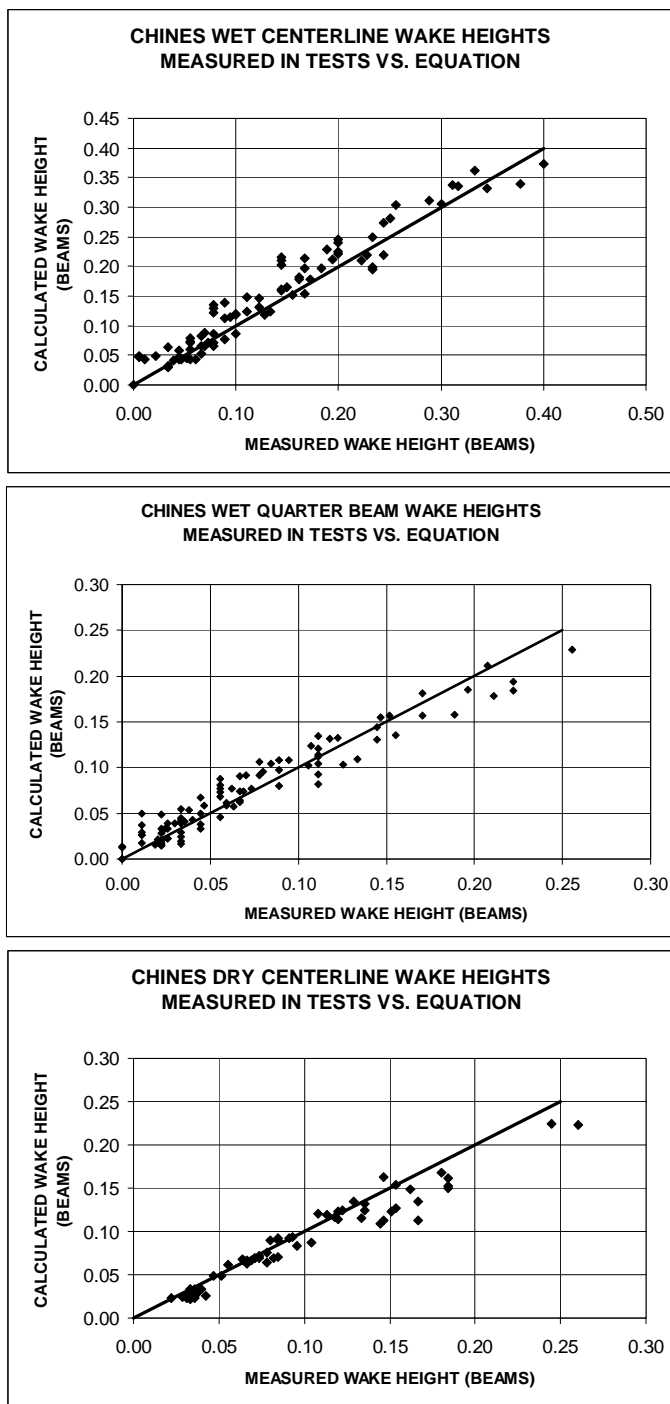


Fig. 15 Plots Showing Goodness of Fit of Wake Equations

Profile Heights at ½ Beam Outboard of Keel It will be noted that while measurements were also made of the longitudinal profiles at a transverse distance of ½ beam outboard of the keel (chine location), they are not presented in this paper. As will be shown in a subsequent section of this paper, for deadrise hulls, where the forebody carries 90% of the total load, the afterbody intersection with the wake occurs primarily along the afterbody keel.

Effect of Deadrise on Wake Profiles It was found that the deadrise angle has a small effect on the longitudinal wake profiles. As shown in the empirical equations, the center-line profiles for the 20° and 30° deadrise hulls were the same (within the scatter of the experimental data). The centerline profiles for the 10° deadrise hull were slightly smaller than those for the larger deadrise hulls. The wake profiles for the ¼ beam buttock reference position were the same for all deadrise angles and were smaller than the center-line profiles. These observations are in general agreement with the conclusions stated in the seaplane wake paper (Korvin-Kroukovsky, Savitsky and Lehman, 1949).

Effect of Wetted Keel Length on Wake Profiles As shown on Figures 9, 10, and 11, for a fixed trim angle and speed, the height of the wake profiles increases with increasing wetted keel length. Since the draft of the keel = $L_k \sin \tau$, it follows that an increase in L_k increases the penetration of the transom relative to the level water line. This in turn increases the hydrostatic pressure at the transom and the volume of the initial cavity generated by the hull. These increased initial disturbances result in larger wake profiles. The reader should remember that the reference lines for the wake profiles shown in this paper are the extension of the keel or ¼ buttock lines from the transom into the wake cavity.

Effect of Trim Angle on Wake Profile As shown on Figures 9, 10, and 11, for a fixed L_k and speed, the height of the wake profiles increases with increasing trim angle. This is a result of the increase in keel draft (as discussed above) and also to an increase in downwash velocity at the transom due to the increasing trim angle. More energy is thus initially imparted to the wake and, as a consequence, the height of the following wake is increased.

For the present test range of trim angles and speed, the wake was observed to be tangent to the hull bottom as it separated from the hull.

Effect of $0.017L_k\tau^{1.5}$ on Wake Profile In developing the empirical equations for wake profile it was found the L_k and τ effects could be well represented by the quantity $0.017 L_k \tau^{1.5}$. The test parameters were such that the minimum value of this quantity was 0.18. Hence the application of the equations is restricted to $0.017 L_k \tau^{1.5}$ values equal to or greater than 0.18.

Effect of Speed Coefficient (C_v) on Wake Profile For otherwise identical planing conditions, increasing C_v “stretches” the longitudinal wake profiles. Thus, at any position X, the wake height decreases with increasing speed coefficient, C_v .

Application of Wake Profiles in Design of Stepped Planing Hulls

To illustrate possible applications of the wake profiles to the design of stepped hulls, the configuration shown on Fig. 3 is used as an example. The principal features of this hull are summarized below:

Total displacement =	10,000 lbs (4546 kg)
LOA =	32ft (9.8m)
Load supported by forebody =	9,000 lbs (4091 kg)
Location of forebody load =	3.5 ft (1.1 m) forward of step
Deadrise angle of forebody =	12.5°
Length of afterbody =	13.5 ft (4.1 m)
Load on afterbody =	1,000 lbs (455 kg)
Deadrise angle of afterbody =	12.5°
Beam of forebody & afterbody =	7.8 ft (2.4 m)
Speed =	40 knots
Speed Coefficient, C_v =	4.3

The objective of this illustration is to define the depth of step and the trim angle of the afterbody relative to the forebody for two possible operating conditions:

1. The aft end of the afterbody intersects the wake and develops the afterbody load and center of pressure position required to provide for vertical equilibrium. In the present illustration the required afterbody load is 1,000 lbs.
2. The afterbody is clear of the wake. In this case the afterbody load will be developed by submerged or

surface piercing adjustable lifting hydrofoil that is attached to the stern.

Using published planing hull performance prediction methods, such as shown in Savitsky (1964), the equilibrium trim angle and wetted keel length of the forebody are readily calculated based on the loading and speed defined above. The results are:

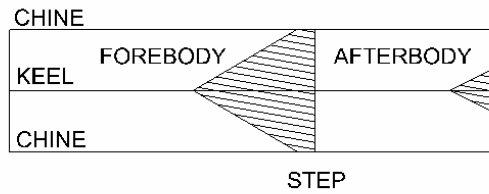
$$\begin{aligned}L_k &= 1.1 \text{ beams} \\L_c &= 0.12 \text{ beams} \\ \tau &= 4.3^\circ \\ C_v &= 4.3\end{aligned}$$

Using these inputs and the wake equations developed in this paper, the longitudinal centerline wake profile can be defined and is plotted on Figures 16 and 17. Note that the vertical scale is substantially larger than the horizontal scale. This was done to more clearly demonstrate the longitudinal curvature of the wake profiles.

The two illustrative cases are discussed as follows:

Afterbody Intersecting Wake Profile (Fig. 16) The procedure consists in first locating the forward keel end of the afterbody at a sufficient distance above the forebody keel (called the step depth) to allow the atmospheric air to proceed downward from the chine to the keel. This will assure ventilation of the flow as it separates from the forebody. Based on many experimental studies of stepped seaplane hulls it was found that a step depth of approximately 5% of the beam would be sufficient to assure natural separation of the flow. Artificial aeration injected through the hull bottom just aft of the step should also be considered since it can promote flow separation. This will reduce the required step height and, as a consequence, reduce the hull drag at non-planing speeds.

PLAN VIEW



H = HEIGHT ABOVE
EXTENDED KEEL
BEAMS

NOTE:

AMPLIFIED VERTICAL
SCALE

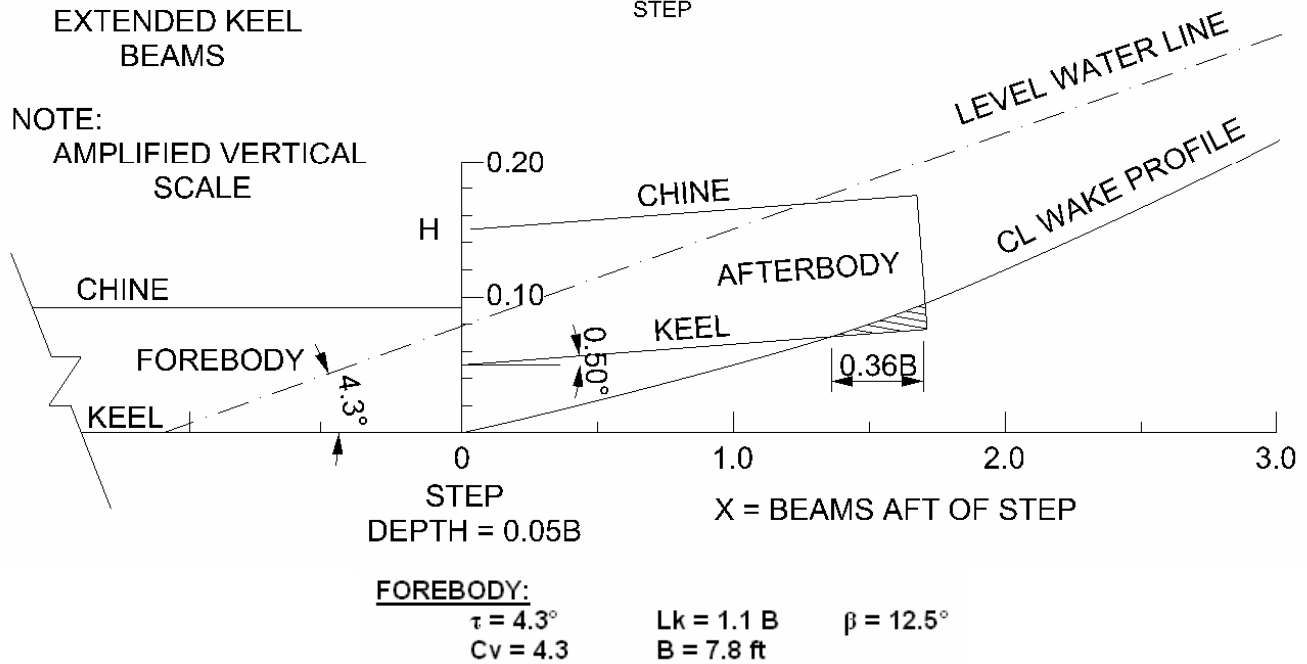


Fig. 16 Stepped Hull (See Fig. 5b) Afterbody Orientation Relative to Wake Profile to Provide 1,000 lb (455 kg) of Lift

The next step is to orient the trim angle of the afterbody relative to the forebody so that its after end intersects the wake and establishes a small lifting area. The extent of the lifting area is related to the afterbody trim angle and thus, defines the load on the afterbody. The quantitative relation between afterbody trim angle and afterbody wetted area is established by superposing the profile of the afterbody on to the wake profile (as shown in Fig. 16) and measuring the wetted keel length for different trim angles. These inputs are used to calculate the afterbody load.

Unfortunately, at this time there is no verified analytical method for calculating the lift force on a hull planing on the surface of the wake profile. Until further studies are carried out, it is suggested that established planing lift equations be used with the added condition that the vertical velocity of local free surface wake profile be included when defining the effective trim angle of the afterbody. This vertical velocity is directly related to the slope of the wake contour at its intersection with the afterbody.

(a) For the case when the afterbody wetted area includes chine wetting, the following lift equations can be used:

$$C_{L\alpha} = \tau^{1.1} (0.0120 \lambda^{1/2} + 0.0055 \lambda^{5/2} / C_v^2) \quad (1)$$

$$C_{L\beta} = C_{L\alpha} - 0.0065 \beta C_{L\alpha}^{0.60} \quad (2)$$

(b) For the case when the afterbody chines are not wetted,

The planform of the wetted bottom area has a triangular shape such as shown on Fig.16. This makes it amenable to simple two dimensional analytical treatments such as developed by Milwitzky (1948). While that study deals with the impact of chines-dry prismatic hulls on a level water surface, the results are readily adaptable to the steady planing process by eliminating the impact acceleration terms. The following equation for the planing lift of a chines-dry prismatic hull is thus developed

$$C_L = W / \frac{1}{2} \rho V^2 L_k^2 \quad (10)$$

$$C_L = \pi (\pi / 2\beta - 1)^2 \sin^3 \tau [(1 - \tan \tau / 2 \tan \beta)] \quad (11)$$

The term just ahead of the brackets represents the results of the two dimensional flow analysis. The term in the brackets is the correction for end flow losses due to the finite aspect ratio of the triangular plan form. Milwitzky states that these functions are in good agreement with the experimental data for deadrise angles of 22.5, 30 and 40 degrees and “may not be too far in error for angles as low as 15 deg.”

For the present illustrative example, it was found that the afterbody intersection with the wake resulted in a chines-dry wetted bottom area. Also an afterbody trim angle of 0.50°.

relative to the forebody resulted in a wetted keel length of 2.8 ft. This is shown on Fig. 16. The hydrodynamic trim angle of this area is a combination of forebody trim, afterbody trim relative to the forebody and the local vertical velocity of the rising surface profile of the wake in the wetted bottom region. This vertical velocity is of course related to the surface wave slope. For the present case, as can be seen in Fig. 16, the local slope of the wake contour is essentially parallel to the free water surface so that there is no vertical component of velocity due to the wake. These components result in an effective local hydrodynamic trim angle of the afterbody of 3.8° . Substituting these values into the chines-dry lift equation results in an afterbody load of approximately 1080 lbs. Assume that the center of pressure of this load is $0.40 L_K$ forward of the transom. (1.1 ft. forward of the stern). It will be recalled that an afterbody load of 1,000 lbs and a longitudinal position of its center of pressure 1 ft forward of the transom was required for vertical equilibrium. Further iteration of the trim angle of the afterbody will result in a keel length that provides the required values of load and center of pressure. Unfortunately, the present experimental set-up did not provide means for measuring the afterbody load, hence comparison with equation 11 was not possible.

The relatively small calculated triangular shaped wetted bottom area at the stern of the deadrise afterbody is limited to the keel region. Hence the longitudinal wake profile along the forebody centerline is of primary importance in defining the afterbody interference with the wake. Fig. 17 is an underwater photograph of a typical stepped planing hull. The small triangular shaped afterbody wetted bottom is clearly evident.

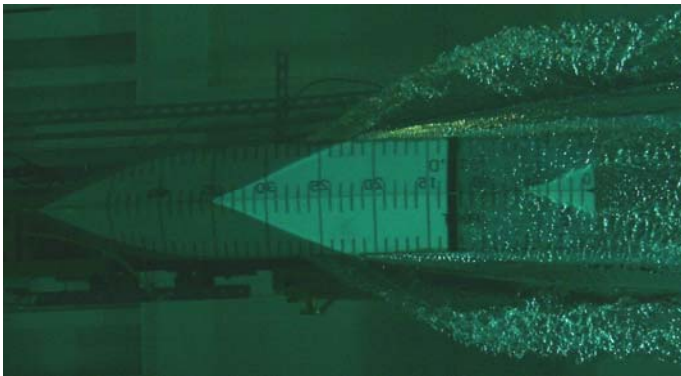


Fig. 17 Wetted Areas for Typical Stepped Hull

Afterbody Clear of Wake (Fig. 18) It may well be that, in the above illustrative example, the attempt to obtain vertical equilibrium by using the afterbody load may not be a stable solution. The uncertainty is associated with the relatively small afterbody wetted area and the small wetted keel length, L_k . Since the load varies as the square of L_k , small perturbations in

wetted length may produce significant perturbations in this load and thus result in longitudinal instability. Further, as the speed varies, the extent of the afterbody wetted area and its lift force will also vary. It may well be that longitudinal equilibrium may not be attainable over the operating speed range. This possibility should be studied.

A possible solution to this uncertainty is to trim the afterbody so that it is entirely clear of the wake. The vertical force required for equilibrium can be provided by a small, adjustable, submerged or surface piercing hydrofoil that is attached to the stern of the afterbody. The angle of attack of this foil can be adjusted to provide the lift force required for vertical equilibrium at each speed. Its pitch moment arm relative to the LCG is independent of the wake slope. In addition, the hydrofoil will also provide pitch damping to attenuate any porpoising tendency. Fig. 18 shows such an arrangement. The afterbody is now oriented at a trim angle of 2.0° relative to the forebody.

Designers of stepped planing hulls may find alternate ways to incorporate these wake profiles into their design. They are encouraged to do so. What is presented herein is just one possible application that is intended to illustrate a possible methodology.

Spray Pattern When the Stagnation Line Crosses the Step

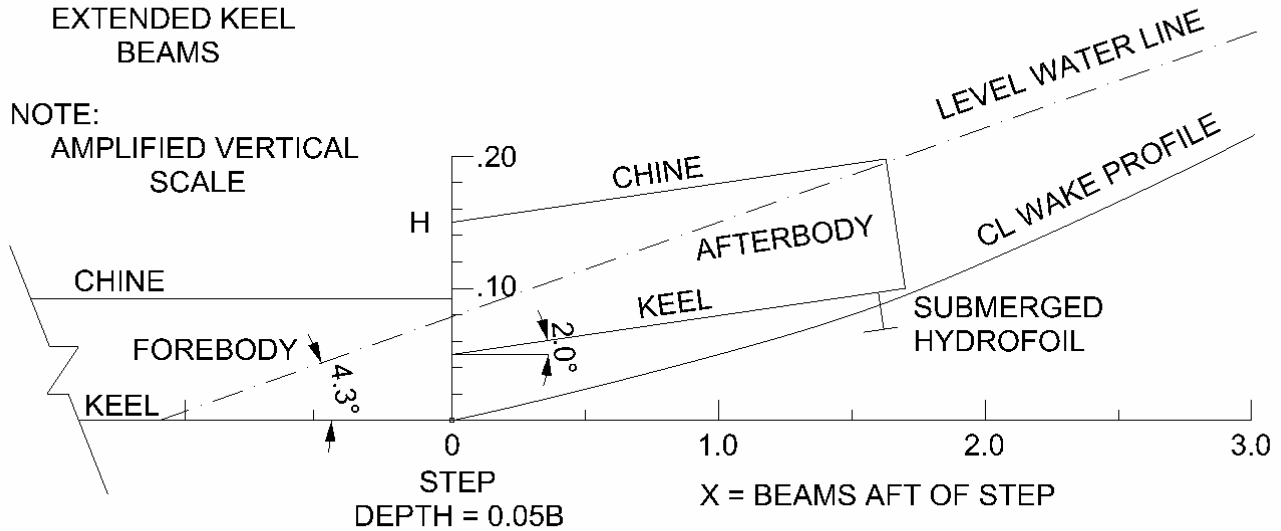
This paper emphasized the importance of designing a stepped planing hull so that the forebody chines are always wetted (stagnation line crosses the chine). To accomplish this, it has been recommended that the wetted chine length be at least 0.10 beams. If the stagnation lines do cross the step, large, high velocity, spray sheets originate at these intersection points and impact against the bottom of the afterbody. This will result in a large increase in total resistance and possibly initiate longitudinal instability. Water-based aircraft commonly observe these effects during take-off since the stagnation line must cross the step just prior to the aircraft becoming airborne.

In some designs it may not be feasible to achieve chine wetting at high speed. Hence several runs were deliberately made with the stagnation lines crossing the transom of the test model. Fig. 19 is a photograph of the spray pattern associated with this planing condition. Although measurements were not made of the spray height or intensity, the photograph does clearly demonstrate the severity of this spray. Measurements were made of the longitudinal centerline surface wave profile in the wake. It was found that the data are also well represented by empirical equations similar to those for the chines wetted case. These are equations 12-14.

H = HEIGHT ABOVE
EXTENDED KEEL
BEAMS

NOTE:

AMPLIFIED VERTICAL
SCALE



FOREBODY:

$$\tau = 4.3^\circ$$

$$C_v = 4.3$$

$$L_k = 1.1 B$$

$$B = 7.8 \text{ ft}$$

$$\beta = 12.5^\circ$$

Fig. 18 Stepped Hull (see Fig. 5b) Afterbody Orientation Relative to Centerline Wake Profile to Avoid Afterbody Wetting

Centerline Profile:

$$\beta = 10^\circ$$

$$H = 0.17 [1.5 + 0.03 L_k \tau^{1.5}] \text{Sin} \left[\frac{\pi}{C_v} \left(\frac{X}{3} \right)^{1.5} \right] \quad (12)$$

$$\beta = 20^\circ$$

$$H = 0.17 [1.5 + 0.03 L_k \tau^{1.5}] \text{Sin} \left[\frac{\pi}{C_v} \left(\frac{X}{3} \right)^{1.5} \right] \quad (13)$$

$$\beta = 30^\circ$$

$$H = 0.17 [1.0 + 0.03 L_k \tau^{1.5}] \text{Sin} \left[\frac{\pi}{C_v} \left(\frac{X}{3} \right)^{1.5} \right] \quad (14)$$

* In this chines dry case B = actual wetted beam width in contrast to the geometric beam used in the chines wetted equations. It is used to non-dimensionalize L_k , C_v , and X.

Fig. 20 illustrates the additional afterbody wetting due to the forebody stagnation line intersecting the step. The wetting due to the intersection with the forebody wake was calculated and is identified separately on Fig. 20. The additional wetting due to the spray cones originating at the stagnation lines with the step is also shown and was obtained from an underwater photograph of a stepped hull. Note the large increase in afterbody wetted area due to the spray wetting. This emphasizes the need to design a chine wetted forebody for stepped hulls to avoid large increases in hydrodynamic resistance.



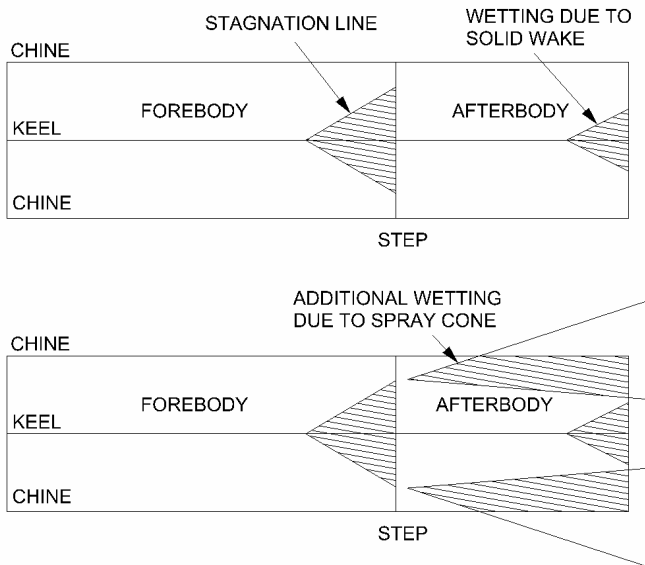
20° with Wetted Beam = 61% Chine Beam



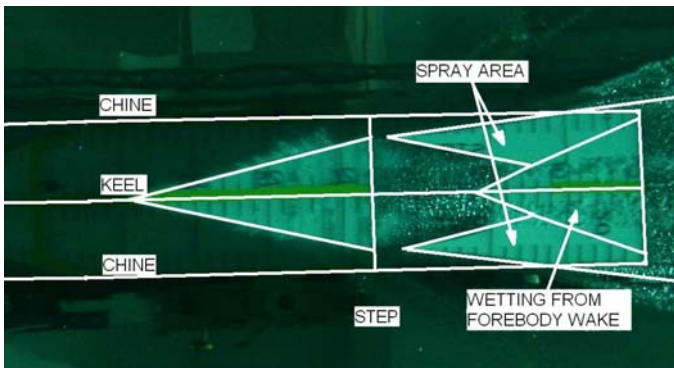
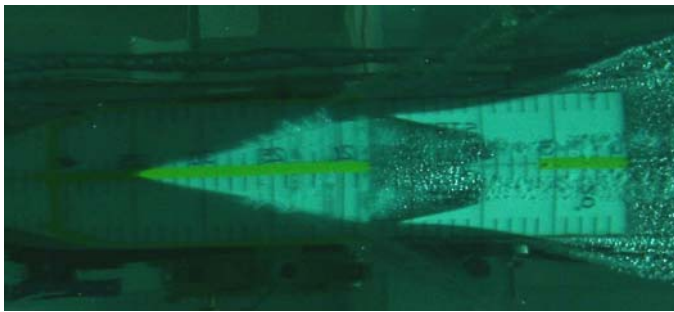
30° with Wetted Beam = 58% Chine Beam

Fig. 19 Spray Patterns Associated with Stagnation Line Intersecting Step

Note: The height highlighted on the photos is the height from the undisturbed water surface to the top of the spray



Sketch of Wetted Areas Due to Solid Wake and Due to Spray Cone



Under Water Photograph of Chines Dry Run, and same photograph with areas highlighted

Fig. 20: Additional Afterbody Wetting Due to Chines Dry Forebody Spray

CONCLUSIONS

The ubiquitous monohull configuration of planing hulls has inherently large drag/lift ratios at very high planing speeds. It is demonstrated that this deficiency can be overcome by the use of stepped hulls. A complete design of stepped hulls however requires a knowledge of the wake form developed by the

forebody upon which the afterbody planes. Unfortunately, there has been a dearth of published data defining these surface wake contours. The present study fills this void by presenting the results of an extensive series of model tests to measure the surface wake profiles for several prismatic planing hulls over a range of test parameters typical for high speed stepped hulls. Empirical equations are developed that represent the longitudinal surface profiles of the wake at various lateral distances from the model centerline. These equations can be easily evaluated for specified operating conditions of a stepped planing hull.

Two illustrative examples are presented that demonstrate a methodology for combining the wake form with established planing lift equations to properly orient the afterbody relative to the forebody and its wake profile so that both longitudinal equilibrium and maximum hydrodynamic lift/drag ratios are attained. It is demonstrated that this single stepped hull has a hydrodynamic drag approximately $\frac{1}{2}$ that of an equivalent monohull at high speeds. This presentation is intended to demonstrate to designers the ease and simplicity of using these wake data to complete their designs.

Although five longitudinal surface wake profiles were obtained, it is shown that the most relevant for deadrise hulls is the longitudinal profile aft of the forebody keel centerline.

The report also demonstrates the substantial increase in afterbody wetted area associated with the forebody stagnation line intersecting the step (the so-called chines dry planing condition).

ACKNOWLEDGMENT

The authors are indebted to the T&R Steering Committee of the Society of Naval Architects and Marine Engineers for their encouragement to undertake this study and for providing partial financial support. We also thank Stevens Institute of Technology for the use of the Davidson Laboratory towing tank and undergraduate students, Maggie Hayes, Eric Giesberg and Kyle Manning, who enthusiastically assisted in all phases of this study.

REFERENCES

- CLEMENT, E.P. and KOELBEL, J.G., Jr. "Optimized Designs for Stepped Planing Monohulls and Catamarans." HPMV-92, Intersociety High Performance Marine Vehicles and Exhibit, Washington D.C., June, 1992
- JOHNSON, V.E., Jr. "Theoretical and Experimental Investigation of Supercavitating Hydrofoils Operating Near the Free Water Surface." NASA Technical Report R-93, 1961.

KORVIN-KROUKOVSKY, B.V., SAVITSKY, DANIEL and LEHMAN, W.F. "Wave Contours in the Wake of a 20-degree Deadrise Planing Surface." Davidson Laboratory, Stevens Institute of Technology Report R-337, June, 1948a.

KORVIN-KROUKOVSKY, B.V., SAVITSKY, DANIEL and LEHMAN, W.F. "Wave Contours in the Wake of a 10-degree Deadrise Planing Surface." Davidson Laboratory, Stevens Institute of Technology Report-R-344. November, 1948b

KORVIN-KROUKOVSKY, B.V., SAVITSKY, DANIEL and LEHMAN, W.F. "Wave Profile of a VEE Planing Surface, Including Test Data on a 30-degree Deadrise Surface." Davidson Laboratory, Stevens Institute of Technology Report R-339, April, 1949.

MACPHAIL, D.C. and TYE, W.D. "The Waves Close Behind a Planing Hull." Royal Aircraft Establishment, Farnborough Report No. Aero, 1992. November, 1944.

MILWITZKY, B. "A General Theoretical and Experimental Investigation of Motions and Hydrodynamic Loads Experienced by V-Bottom Seaplanes during Step-Landing Conditions." NACA Technical Note No. 1516. Washington DC, February 1948

SAVITSKY, DANIEL "Hydrodynamic Design of Planing Hulls." SNAME-MARINE TECHNOLOGY Vol.1, No.1, Oct. 1964, pp 71-95

SAVITSKY, DANIEL, AND BROWN, P.W. "Procedures for Hydrodynamic Evaluation of Planing Hulls in Smooth and Rough Water" SNAME Marine Technology, Vol.13, No. 4, Oct. 1976, pp 381-400

SAVITSKY, DANIEL, DELORME, M. F. and DATLA, R., "Inclusion of Whisker Spray in Performance Prediction Method for High Speed Planing Hulls." SNAME Marine Technology, Vol.44, No.1, Jan. 2007, pp 35-5

SHOEMAKER, J. "Tank Tests of Flat and V-bottom Planing Surfaces." NACA Technical Note No.509. 1934

SOTTORF, W. "Experiments with Planing Surfaces." NACA Technical Memorandum No. 739, March 1934.

VAN DYCK, R. "Final Engineering Report On Wake-Shapes of Planing Forms Associated With High-Speed Water Based Aircraft" Davidson Laboratory, Stevens Institute of Technology Report R-768, October, 1960.

NOMENCLATURE

C_{L_0} = lift coefficient, zero deadrise
 $\Delta / 0.50 \rho V^2 B^2$
 $C_{L\beta}$ = lift coefficient, deadrise surface
 $\Delta / 0.50 \rho V^2 B^2$
 C_v = speed coefficient
 $V / (gB)^{1/2}$
 C_Δ = load coefficient
 $= \Delta / w B^3$
 C_f = friction coefficient
 $= R_f / 0.50 \rho V^2 S$
 L_k = wetted keel length, beams
 L_c = wetted chine length, beams
 λ = mean wetted length/beam ratio
 $(L_k + L_c) / 2$
 Δ = displacement, lbs

Δ_f = load on forebody, lbs
 W = load on afterbody, lbs
 B = chine beam, ft
 S = wetted area, ft²
 τ = trim angle, degrees
 β = deadrise angle, degrees
 X = distance aft of step, beams
 H = height of wake profile above extended forebody bottom, beams
 T = time, sec.
 R_T = total resistance, lbs
 R_f = viscous resistance, lbs
 V = velocity, ft/sec
 σ = flap deflection, degrees
 ∇ = displaced volume, ft³
 F_∇ = Volumetric Froude Number
 $V / (g\nabla^{1/3})^{1/2}$